Bull Soc Chim Fr (1997) 134, 471-486
© Elsevier, Paris

Synthesis and characterization of unsymmetrical *cis*-(phosphino-phospholyl)ethene tetracarbonyl molybdenum complexes: hydrophosphination reactions of $(HC{\equiv}CCH_2PPh_2)Mo(CO)_5$ and $(HC{\equiv}CCH_2DBP)Mo(CO)_5$

Kalyani Maitra, Vincent J Catalano, John H Nelson*

Department of Chemistry, University of Nevada, Reno, Nevada 89557-0020, USA

(Received 15 November 1996; accepted 6 March 1997)

Summary — The base-catalyzed hydrophosphination reactions of $(HC{\equiv}CCH_2PPh_2)Mo(CO)_5$ and $(HC{\equiv}CCH_2DBP)Mo(CO)_5$ with $(Ph_2PH)Mo(CO)_5$ and $(DBPH)Mo(CO)_5$ give several different products as a function of reaction conditions. These products were characterized by elemental analyses, physical properties, ^1H, $^{13}C\{^1H\}$, and $^{31}P\{^1H\}$ NMR spectroscopy, infrared spectroscopy, and in several cases by X-ray crystallography.

diphosphine / hydrophosphination / molybdenum complex

Résumé — Synthèse et caractérisation de complexes asymétriques *cis*-(phosphino-phospholyl)éthène tétracarbonyl molybdène : réactions d'hydrophosphination de $(HC{\equiv}CCH_2PPh_2)Mo(CO)_5$ et $(HC{\equiv}CCH_2DBP)Mo(CO)_5$. La réaction d'hydrophosphination de $(HC{\equiv}CCH_2PPh_2)Mo(CO)_5$ et de $(HC{\equiv}CCH_2DBP)Mo(CO)_5$ avec $(Ph_2PH)Mo(CO)_5$ et $(DBPH)Mo(CO)_5$ donne divers produits en fonction des conditions réactionnelles. Ces produits ont été caractérisés par analyse élémentaire, par leurs propriétés physiques, par spectroscopie RMN de ^1H, ^{13}C et ^{31}P, spectroscopie infrarouge et, dans plusieurs cas, par radiocristallographie aux rayons X.

diphosphine / hydrophosphination / complexe de molybdène

Introduction

Coordination of a phosphinoalkyne to a transition metal through the phosphorus atom greatly modifies the reactivity of the alkyne functionality activating it toward such reactions as hydration [1], hydrogen halide [2] addition and acetylene coupling [3]. Analogous activation toward addition of the P–H moiety (hydrophosphination) of secondary phosphines gave stereospecifically the *cis*-1,2-diphosphinoalk-1-ene complexes (equation (1)) [4]. Such addition reactions of secondary phosphines to activated carbon–carbon multiple bonds provide an efficient route for the syntheses of unsymmetrical, rigid, chelating tertiary diphosphine ligands which have potential applications in the area of asymmetric catalysis [5]. Previously, as part of our extensive studies into these reaction types, we reported the formation of the chelate diphospholyl and diphosphine complexes **A** [6] and **B** [7], respectively. The reaction of the secondary phosphole complex $(HDBP)Mo(CO)_5$ (**1b**) with the alkyne phosphole complex $(HC{\equiv}CCH_2DBP)Mo(CO)_5$ (**2b**) gave complex **A** (equation (2)) [6]. Similarly, complex **B** was prepared by the base-catalyzed hydrophosphination reaction of the alkyne phosphine complex $(HC{\equiv}CCH_2PPh_2)Mo(CO)_5$ (**2a**) with the secondary phosphine complex $(HPPh_2)Mo(CO)_5$ (**1a**) as shown in equation (3) [7].

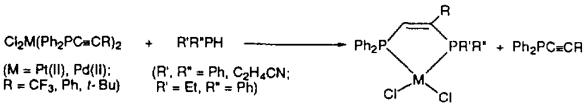

(1)

For both the above reactions the use of the coordinated secondary phosphine and phosphole avoids the difficult preparation and handling of free secondary phosphines and also has greater atom economy compared to the method described in equation (1).

We now describe the reactions of the coordinated secondary phosphine/phosphole with the coordinated tertiary phosphole/phosphine, containing an activated acetylene unit. In this way complexes of mixed unsymmetrical *cis*-(phosphino or phospholyl) ethenes analogous to **A** and **B** have been prepared.

---

* Correspondence and reprints

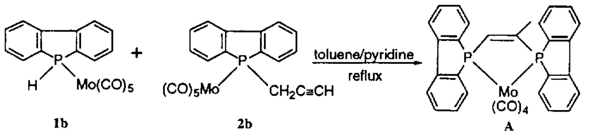

(2)

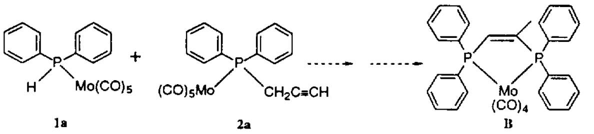

(3)

Results and discussion

The 1:1 reaction of **1a** with **2b** in the presence of KOBu^t in refluxing THF gave complexes **3a**, **4a**, **5a** and **7** in the crude reaction mixture. These compounds were separated by column chromatography followed by recrystallization from a 1:1:1 mixture of dichloromethane / ether / methanol (scheme 1).

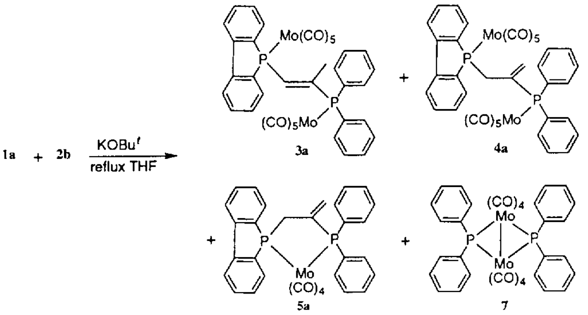

Scheme 1

The base-promoted addition of the P–H bond in complex **1a** across the acetylenic moiety of **2b** occurs in the Markovnikov sense to produce **4a**, as shown by the presence of the two geminal vinyl proton resonances in the ^{1}H NMR spectrum. The column fraction which contained complex **4a** was contaminated with a considerable amount of complex **7** and almost equal amounts of three other species that were only characterized by $^{31}\text{P}\{^1\text{H}\}$ NMR spectroscopy [δ 34.0, 28.1 (J_{PP} = 6.5 Hz); δ 49.9, 28.1 (J_{PP} = 5.5 Hz); δ 68.8, 51.8 (J_{PP} = 5.7 Hz)]. The dark red complex **7** was isolated by repeated recrystallization of these column fractions. Earlier [7], we reported the formation of **7** under similar reaction conditions and completed its structural characterization by NMR, IR spectroscopy and X-ray crystallography. Multiple attempts to purify **4a** by fractional crystallization or column chromatography employing different solvent systems failed to give the pure compound. Recrystallization from a 1:1:1 mixture of dichloromethane / ether / methanol afforded large pale yellow-green prolate spheroid crystals along with some amorphous powdery material. X-ray crystallography of a single crystal taken from this mixture confirmed the presence of **4a** as one of the components. A tedious effort of hand-picking a few of the large crystals having the same morphology enabled us to unambiguously characterize **4a** by ^{1}H, $^{31}\text{P}\{^1\text{H}\}$, $^{13}\text{C}\{^1\text{H}\}$ NMR and IR spectroscopy. The base-catalyzed migration of the double bond in **4a** by a [1,3] hydrogen shift gives the thermodynamically stable *trans*-diphosphine species **3a**. We previously reported the base-catalyzed isomerization of the propargyl complex **2a** [8] in refluxing THF to a mixture of all three isomers **2a**, **2a′** and **2a″** (propargyl, allenyl and propynyl, respectively) in solution. The analogous metal-coordinated DBP-propargyl complex **2b** also undergoes isomerization to **2b′** and **2b″** under the same reaction conditions [8]. Hence **3a** and **4a** could also result from hydrophosphination of the P–H bond in **1a** in Markovnikov's sense across the terminal and internal vinyl functionalities respectively of the DBP-allenyl isomer **2b′**. Similarly, the addition of complex **1a** to the DBP-propynyl isomer **2b″** could result in the formation of the dimolybdenum *trans*-di(phosphinophospholyl) product **3a**. We have seen earlier [7] that under similar reaction conditions, the diphenyl propynyl isomer **2a″** is less reactive towards the hydrophosphination reaction and, if formed, was recovered from the product mixture. We have not been able to isolate the analogous DBP-propynyl isomer **2b″** from the mixture of products. It is quite possible that some of the impurities present in the fractions which eluted complex **4a** may contain some of the rearranged isomer **2b″** which we were unable to isolate. The $^{31}\text{P}\{^1\text{H}\}$ NMR spectra of **3a** and **4a** each show the presence of a pair of inequivalent ^{31}P nuclei with $^3J_{\text{PP}}$ values of 22.5 Hz and 6.08 Hz respectively. The *trans* orientation of the two phosphorus nuclei across the double bond in **3a** enhances the coupling constant value through conjugation, and the value is higher than that observed for **4a**. Previously, we have reported evidence for the formation of the analogous diphosphine [7] and diphosphole [6] complexes of the type **4a** resulting from the addition of the P–H bond

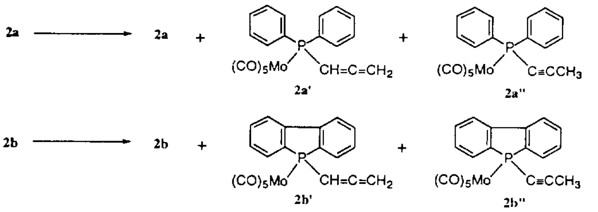

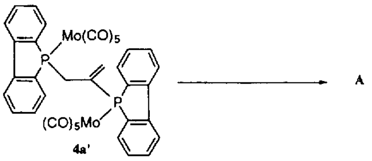

(4)

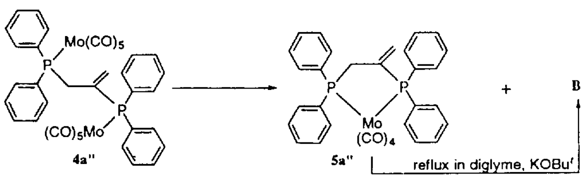

(5)

in Markovnikov's sense in the reactions of **1a** with **2a** or **1b** with **2b**, respectively. These analogs **4a′** and **4a″** could be efficiently converted to the chelate complexes **A** and **B** respectively, as shown in equations (4) [6] and (5) [7] above. In the latter case the *exo*-methylene chelate intermediate **5a″** was also formed, and it underwent isomerization to **B** as the final product. We were unable to isolate a sufficient amount of pure **4a** to enable separate verification of its conversion to **5a** or **6a**. Still, it may be concluded that the conversion pathway will most likely be the same as that shown for its phosphine and phosphole analogs (equations (4) and (5)). Moreover, **4a** may be a very reactive intermediate that readily converts either to complex **5a** or **3a** and hence would be detected in small quantity in the product mixture. Suggestively, the driving force of chelation caused **4a** to undergo thermally induced Mo(CO)$_6$ elimination to produce the exo-methylene chelate diphosphine or rather the mixed phoshine–phospholyl complex **5a** (scheme 1). The latter underwent base-catalyzed isomerization in refluxing diglyme to give the thermodynamically stable *cis*-isomer **6a** in near quantitative yield (scheme 2).

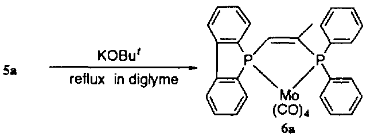

Scheme 2

The $^{31}\mathrm{P}\{^1\mathrm{H}\}$ NMR spectra of complexes **5a** and **6a** show the presence of two inequivalent phosphorus nuclei (δ 34.13, 54.79, **5a**; 46.88, 72.82, **6a**) in each case with $^2J_{\mathrm{PP}}$ values of 8.39 Hz and 4.62 Hz respectively. The downfield shifts of the ^{31}P resonances of **5a** and **6a** compared to those of **4a** (δ 28.04, 51.27) are consistent with the formation of the five-membered chelate ring [9]. The small values of $^2J_{\mathrm{PP}}$ are also typical of five-membered chelate rings on Mo(0) [10].

The ^{1}H NMR spectrum of **5a** showed resonances for the two geminal vinyl protons and two methylene protons while for **6a** only one vinyl proton and a methyl resonance were observed. These observations are consistent with the base-promoted [1, 3] migration of a methylene proton to the terminal vinyl carbon [11, 12] and isomerization of the carbon–carbon double bond to give exclusively the thermodynamically more stable *Z*-isomer. In the $^{13}\mathrm{C}\{^1\mathrm{H}\}$ NMR spectra of both the above complexes the observation of two doublet of doublet resonances for two of the carbonyl carbons in each case indicates the presence of two magnetically inequivalent phosphorus nuclei that are respectively *trans* and *cis* to these two carbonyl groups. This is further confirmed from values for the phosphorus–carbon coupling constants ($^2J_{\mathrm{PC}}$) of 25.09 Hz, 8.3 Hz; 24.39 Hz, 8.93 Hz and 26.21 Hz, 7.61 Hz; 23.70 Hz, 8.49 Hz for **5a** and **6a** respectively. The higher $^2J_{\mathrm{PC}}$ values correspond to the *trans* coupling while the smaller values are due to the *cis* coupling.

A similar hydrophosphination reaction of the secondary phosphole complex **1b** with the tertiary phosphino alkyne complex **2a** in the presence of a catalytic amount of KOBu^t in refluxing THF gave complexes **3b** and **5b** as the major separable products (scheme 3). Minor quantities of complexes **4b**, **8** and **9** were also detected in some of the column fractions by $^{31}\mathrm{P}\{^1\mathrm{H}\}$ and ^{1}H NMR spectroscopy. We were unable to isolate **4b** in a pure form from the mixture of **3b** and other trace impurities to complete its spectral characterization. A $^{31}\mathrm{P}\{^1\mathrm{H}\}$ NMR spectrum for the fraction that contained **4b** as the major species showed the presence of two inequivalent phosphorus atoms [δ 24.8 (P$_\mathrm{A}$), 41.6 (P$_\mathrm{X}$)], with a $^3J_{\mathrm{PP}}$ value of 6.87 Hz and the following minor resonances at : δ 46.3, 44.7 (J_{PP} = 34.7 Hz); δ 46.1, 6.1 (J_{PP} = 33.9 Hz); δ 45.7, 43.1 (J_{PP} = 5.5 Hz). A ^{1}H NMR spectrum for **4b** showed resonances for the two methylene protons at δ = 2.78 (apparent triplet, $^2J_{\mathrm{PH}} = {}^3J_{\mathrm{PH}}$ = 5.13 Hz), and for the two vinyl protons at δ = 5.80 (d, $^3J_{\mathrm{PH}}$ = 45.41 Hz) and δ = 6.20 ($^3J_{\mathrm{PH}}$ = 22.46 Hz) respectively. Hence, based on the ^{1}H and $^{31}\mathrm{P}\{^1\mathrm{H}\}$ NMR spectroscopic data obtained we were able to identify complex **4b** in the mixture of compounds, and the values obtained are in close agreement with those of its structural analogs **4a**, **4a′** and **4a″**. When the same reaction of **1b** with **2a** was conducted under more forcing conditions, refluxing diglyme, complexes **3b**, **5b** and **9** were formed along with a minor amount of the unexpected product **10** (scheme 4).

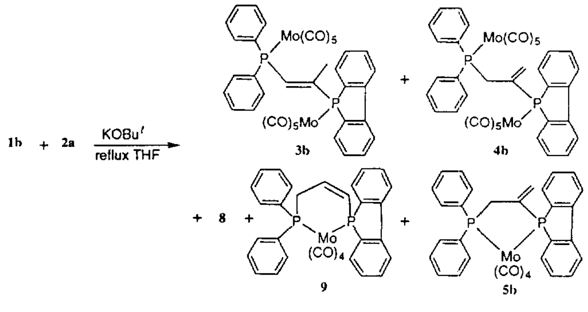

Scheme 3

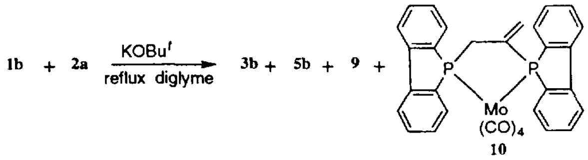

Scheme 4

The explanation for the formation of complexes **3b**, **4b** and **5b** from this hydrophosphination reaction is the same as discussed earlier for their analogs **3a**, **4a** and **5a** respectively. Interestingly, the column fraction which contained complex **5b** showed the presence of the *cis*-chelate isomer **6b** in trace amounts as observed by $^{31}\mathrm{P}\{^1\mathrm{H}\}$ NMR spectroscopy. A possible mechanistic pathway for the formation of the bridged complex **8** is outlined in equation (6). In the first step condensation of two equivalents of the secondary phosphole **1b** in the presence of a base gives the bridged intermediate dimer **8′**, which then reacts with another molecule of **1b** followed by the elimination of Mo(CO)$_6$ to finally produce complex **8** containing a terminally coordinated secondary phosphole. Bridged complexes of the type **8′**

[13, 14] are typically prepared under similar conditions. The structure of **8** was established by ^{31}P{^{1}H} NMR spectroscopy. It shows resonances for the three non-equivalent phosphorus atoms at δ 188.87 (d), 167.90 (d) and -12.01 ppm (apparent triplet) respectively, representing an AMX spin system, having accidentally the same phosphorus–phosphorus coupling constant value of 34.09 Hz. The chemical shift at $\delta = -12.01$ ppm can readily be assigned to the phosphorus atom of the secondary phosphole. Moreover, in the ^{31}P NMR spectrum with selective proton decoupling the upfield phosphorus resonance is a doublet ($^{1}J_{\mathrm{PH}} = 349.47$ Hz) of apparent triplets due to coupling to the other two bridging phosphorus nuclei. This confirms the presence of the coordinated secondary phosphole. A single crystal X-ray diffraction study further confirmed the structure of **8**. Interestingly, for the reaction performed in diglyme, the column fractions which contained **5b** were contaminated with trace amounts of another phosphido-bridged dimer as evidenced by the three inequivalent phosphorus resonances in the ^{31}P{^{1}H} NMR spectrum (see Experimental section).

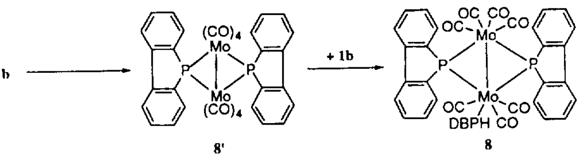

(6)

The formation of complex **9** is unique as it is the first example encountered for the systems yet studied where the addition of the P–H bond to the alkyne moiety occurred in an *anti*-Markovnikov's sense followed by concomitant elimination of $\mathrm{Mo(CO)_6}$ to give the six-membered chelate ring. Complex **9** was obtained in higher yield under harsher reaction conditions (scheme 4). The ^{31}P{^{1}H} NMR spectrum of **9** shows the presence of two inequivalent ^{31}P nuclei with a $^{2}J_{\mathrm{PP}}$ value of 32.97 Hz, a typical value for six-membered chelate rings on Mo(0) [9]. The ^{1}H NMR spectrum showed three non-aromatic resonances at $\delta = 3.21$, 5.62 and 6.88 with 2:1:1 relative intensities. From selective proton decoupling of the ^{1}H NMR spectrum the low field resonances at $\delta = 5.62$ and $\delta = 6.88$ were assigned to the $\mathrm{CH_2C}H\!=$ and $\mathrm{CH\!=\!C}H$ protons respectively. The high field resonance at $\delta = 3.21$ was assigned to the methylene protons.

The isolation of complex **10** (scheme 4) as one of the minor products was an unexpected result for the hydrophosphination reaction performed in diglyme. Previously [6], this intermediate *exo*-methylene five-membered chelate complex was not detected as a product from the reaction of **1b** with **2b** in pyridine (equation (2)). It is possible that in diglyme with KOBu^t, the propargyl unit ($-\mathrm{CH_2C{\equiv}CH}$) of the phosphine molecule **2a** replaced the hydrogen of the P–H unit of the secondary phosphole **1b** to produce the propargyl tertiary phosphole complex **2b**, as shown in the following.

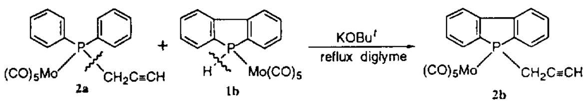

Then complex **2b** underwent hydrophosphination with complex **1b** to give the intermediate complex **4a′** and after thermally induced elimination of $\mathrm{Mo(CO)_6}$ finally produced the bis-(dibenzophospholyl) *exo*-methylene chelate complex **10**. The structure of complex **10** was established by ^{1}H, ^{31}P{^{1}H} and ^{13}C{^{1}H} NMR and IR spectroscopic data. The observation of a two-proton methylene resonance and two geminal vinyl proton resonances in a 2:1:1 ratio in the ^{1}H NMR spectrum is consistent with the structure of **10**.

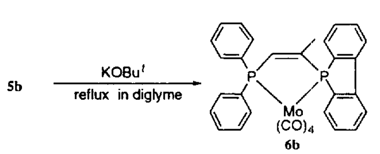

Scheme 5

Complex **5b** underwent KOBu^t-catalyzed isomerization in refluxing diglyme to produce complex **6b** in near quantitative yield (scheme 5). The base-promoted migration of a methylene proton to the terminal vinyl carbon in **5a** drives the stereochemistry of the new carbon–carbon double bond formation giving rise exclusively to the *Z*-isomer, **6b**. The structure of **6b** was established by ^{1}H, ^{31}P{^{1}H} and ^{13}C{^{1}H} NMR and IR spectroscopy and further confirmed by X-ray crystallography.

Interestingly, for the reaction of **1a** with **2b** (scheme 1) the *cis*-chelate isomer **6a** was not detected in the mixture of products. Similarly for the reaction of **1b** with **2a**, performed in diglyme (scheme 4), **6b** could not be isolated even though it was formed in larger quantity than most of the other products as determined by ^{31}P{^{1}H} NMR spectroscopy of the crude product mixture. Conclusively, it appears from the study of these hydrophosphination reactions that the formation of the *cis*-chelate isomers of type **6a** and **6b** is less favored in the first step of the reaction than the formation of the isomeric *exo*-methylene *cis*-chelate complexes **5a** and **5b** which were obtained in good yield. The latter may then be efficiently isomerized in the presence of a base to **6a** or **6b** respectively.

Single-crystal X-ray analyses of complexes **3a**, **3b**, **4a**, **5b**, **6a**, **6b**, **8** *and* **9**

Crystals of all eight compounds mentioned above were grown by slow diffusion of methanol into dichloromethane solutions through an ethereal layer. Each structure consists of isolated molecules with no unusual intermolecular contacts. The crystals of **9** were obtained as a 1:1 dichloromethane solvate and those of **3a** contained one water molecule disordered over three sites. For all these complexes the coordination geometry around the metal centers is a distorted octahedron as is usually observed for molecules of this type [15, 16]. The molecular structures for the isomeric bis(molybdenum pentacarbonyl) complexes **3a**, **3b** and **4a** are shown in figures 1–3 respectively, and selected bond distances and angles are listed in tables I–III respectively. Figures 4–7 show the molecular structures for the three five-membered (**5b**, **6a** and **6b**) and one six-membered (**9**) chelate ring molybdenum tetracarbonyl complexes and selected bond distances and angles are listed in tables IV–VII respectively. The metal–phosphorus bond lengths for these complexes lie within the 2.4718(10)–2.5306(11) Å range, in agreement with other reported values [15, 16]. Previously [8], from structural and spectroscopic data we have concluded that the π-acceptor ability of phosphole ligands (RDBP) is greater than their phosphine congeners ($RPPh_2$). Accordingly, for each of the bis(molybdenum pentacarbonyl) and the chelate tetracarbonyl complexes, the observed DBP–Mo bond distance is always slightly shorter than the Ph_2P–Mo bond. The carbon–carbon distances C11–C12 (1.356(10) Å), C23–C25 (1.329(8) Å) and C19–C20 (1.31(2) Å) in the structures of **3a**, **3b** and **4a** respectively, confirm the presence of double bonds. The bond angles C12–C11–P1, C11–C12–C13 for **3a** and C23–C25–P2, C24–C23–C25 for **3b** are 129.3(6)°, 125.4(7)°and 126.0(5)°, 124.5(6)°, respectively. This signifies that C11, C12 in **3a** and C25, C23 in **3b** are essentially sp^2 hybridized. The same is true for **4a** where the bond angles of 122(2)° (C20–C19–C18) and

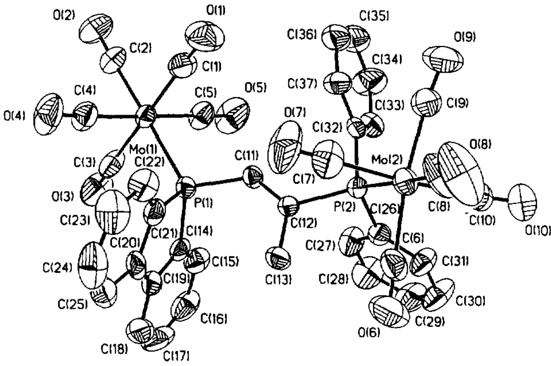

Fig 1. Structural drawing of **3a** showing the atom numbering scheme (40% probability ellipsoids). Hydrogen atoms have been omitted for clarity.

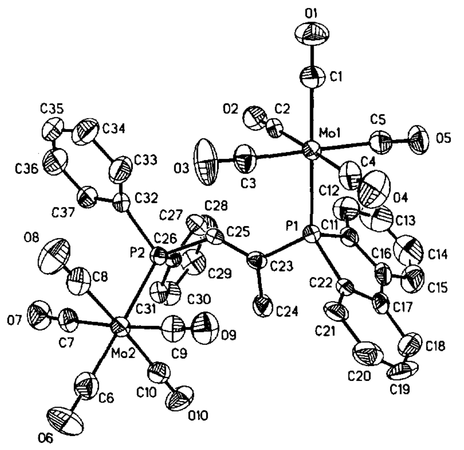

Fig 2. Structural drawing of **3b** showing the atom numbering scheme (40% probability ellipsoids). Hydrogen atoms have been omitted for clarity.

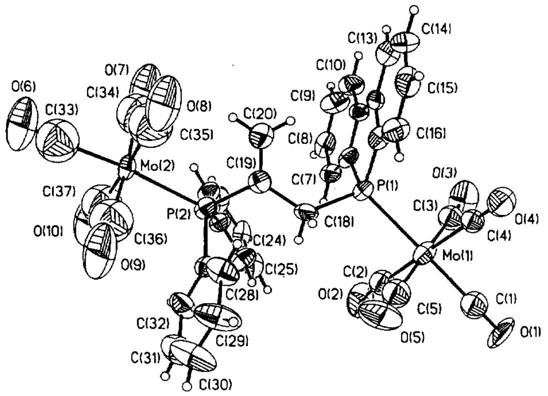

Fig 3. Structural drawing of **4a** showing the atom numbering scheme (40% probability ellipsoids). Hydrogen atoms have an arbitrary radius of 0.1 Å.

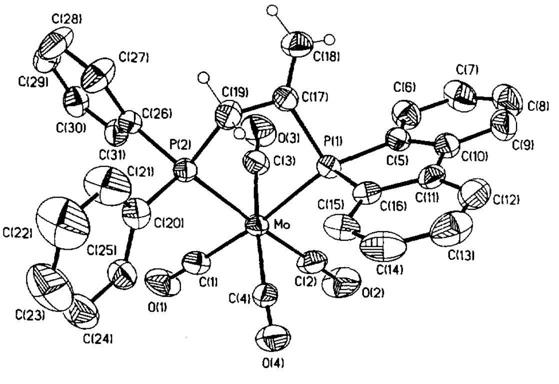

Fig 4. Structural drawing of **5b** showing the atom numbering scheme (40% probability ellipsoids). Hydrogen atoms have an arbitrary radius of 0.1 Å.

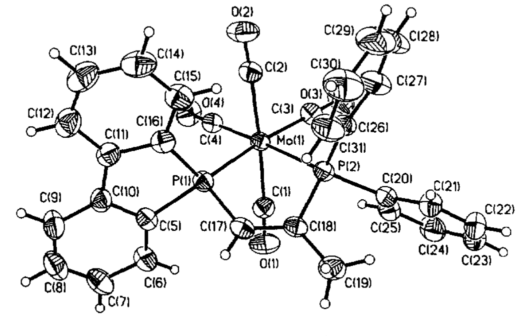

Fig 5. Structural drawing of **6a** showing the atom numbering scheme (40% probability ellipsoids). Hydrogen atoms have an arbitrary radius of 0.1 Å.

Table I. Selected bond lengths and angles for **3a**.

Mo(1)-C(5)	2.002(11)	Mo(1)-C(2)	2.020(10)
Mo(1)-C(4)	2.027(11)	Mo(1)-C(1)	2.042(11)
Mo(1)-C(3)	2.048(12)	Mo(1)-P(1)	2.503(2)
Mo(2)-C(8)	1.972(11)	Mo(2)-C(10)	1.993(12)
Mo(2)-C(9)	2.014(13)	Mo(2)-C(6)	2.023(12)
Mo(2)-C(7)	2.058(14)	Mo(2)-P(2)	2.530(2)
P(1)-C(11)	1.802(8)	P(1)-C(21)	1.821(9)
P(1)-C(14)	1.836(8)	P(2)-C(32)	1.839(8)
P(2)-C(26)	1.840(8)	P(2)-C(12)	1.848(8)
O(1)-C(1)	1.110(12)	O(2)-C(2)	1.117(11)
O(3)-C(3)	1.131(12)	O(4)-C(4)	1.125(12)
O(5)-C(5)	1.139(12)	O(6)-C(6)	1.121(12)
O(7)-C(7)	1.100(14)	O(8)-C(8)	1.118(12)
O(9)-C(9)	1.140(14)	O(10)-C(10)	1.159(12)
C(11)-C(12)	1.356(10)	C(12)-C(13)	1.486(11)
C(5)-Mo(1)-C(2)	91.8(4)	C(5)-Mo(1)-C(4)	179.9(4)
C(2)-Mo(1)-C(4)	88.1(4)	C(5)-Mo(1)-C(1)	89.5(5)
C(2)-Mo(1)-C(1)	89.9(4)	C(4)-Mo(1)-C(1)	90.5(5)
C(5)-Mo(1)-C(3)	89.5(5)	C(2)-Mo(1)-C(3)	90.9(4)
C(4)-Mo(1)-C(3)	90.6(5)	C(1)-Mo(1)-C(3)	178.7(4)
C(5)-Mo(1)-P(1)	90.2(3)	C(2)-Mo(1)-P(1)	177.9(3)
C(4)-Mo(1)-P(1)	89.9(3)	C(1)-Mo(1)-P(1)	89.4(3)
C(3)-Mo(1)-P(1)	89.9(3)	C(8)-Mo(2)-C(10)	89.5(5)
C(8)-Mo(2)-C(9)	86.7(5)	C(10)-Mo(2)-C(9)	83.6(5)
C(8)-Mo(2)-C(6)	87.4(5)	C(10)-Mo(2)-C(6)	91.5(4)
C(9)-Mo(2)-C(6)	172.4(4)	C(8)-Mo(2)-C(7)	88.7(5)
C(10)-Mo(2)-C(7)	175.2(5)	C(9)-Mo(2)-C(7)	91.9(6)
C(6)-Mo(2)-C(7)	92.8(5)	C(8)-Mo(2)-P(2)	174.8(4)
C(10)-Mo(2)-P(2)	95.8(3)	C(9)-Mo(2)-P(2)	94.0(3)
C(6)-Mo(2)-P(2)	92.3(3)	C(7)-Mo(2)-P(2)	86.1(3)
C(11)-P(1)-C(21)	108.7(4)	C(11)-P(1)-C(14)	108.4(4)
C(21)-P(1)-C(14)	91.0(4)	C(11)-P(1)-Mo(1)	112.1(3)
C(21)-P(1)-Mo(1)	117.3(3)	C(14)-P(1)-Mo(1)	117.3(3)
C(32)-P(2)-C(26)	104.5(4)	C(32)-P(2)-C(12)	104.0(3)
C(26)-P(2)-C(12)	99.0(4)	C(32)-P(2)-Mo(2)	113.5(3)
C(26)-P(2)-Mo(2)	119.7(3)	C(12)-P(2)-Mo(2)	114.1(3)
O(1)-C(1)-Mo(1)	179.7(9)	O(2)-C(2)-Mo(1)	178.6(9)
O(3)-C(3)-Mo(1)	176.3(11)	O(4)-C(4)-Mo(1)	177.1(10)
O(5)-C(5)-Mo(1)	178.8(11)	O(6)-C(6)-Mo(2)	175.7(10)
O(7)-C(7)-Mo(2)	179.2(14)	O(8)-C(8)-Mo(2)	177.1(12)
O(9)-C(9)-Mo(2)	173.6(10)	O(10)-C(10)-Mo(2)	176.7(9)
C(12)-C(11)-P(1)	129.3(6)	C(11)-C(12)-C(13)	125.4(7)
C(11)-C(12)-P(2)	120.5(6)	C(13)-C(12)-P(2)	114.0(6)

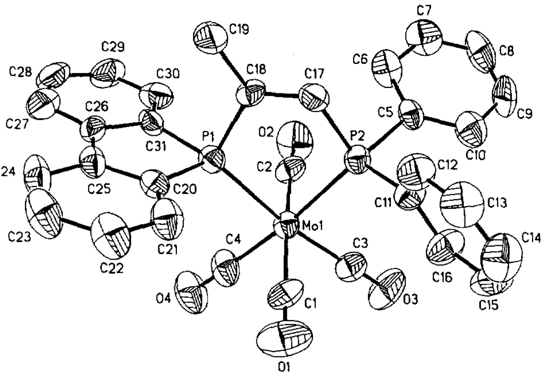

Fig 6. Structural drawing of **6b** showing the atom numbering scheme (40% probability ellipsoids). Hydrogen atoms have been omitted for clarity.

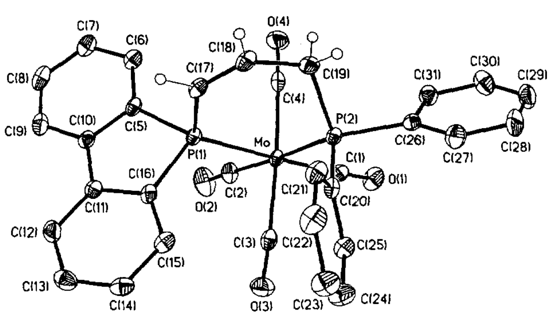

Fig 7. Structural drawing of **9** showing the atom numbering scheme (40% probability ellipsoids). Hydrogen atoms have an arbitrary radius of 0.1 Å.

Table II. Selected bond lengths and angles for **3b**.

Mo(1)–C(1)	1.995(9)	Mo(1)–C(3)	2.029(9)
Mo(1)–C(4)	2.045(9)	Mo(1)–C(5)	2.053(9)
Mo(1)–C(2)	2.059(9)	Mo(1)–P(1)	2.505(2)
Mo(2)–C(6)	1.985(10)	Mo(2)–C(9)	2.006(9)
Mo(2)–C(10)	2.029(9)	Mo(2)–C(8)	2.031(9)
Mo(2)–C(7)	2.034(8)	Mo(2)–P(2)	2.510(2)
P(1)–C(11)	1.811(7)	P(1)–C(22)	1.832(7)
P(1)–C(23)	1.841(7)	P(2)–C(25)	1.818(6)
P(2)–C(26)	1.835(7)	P(2)–C(32)	1.836(7)
O(1)–C(1)	1.144(9)	O(2)–C(2)	1.113(8)
O(3)–C(3)	1.136(9)	O(4)–C(4)	1.122(9)
O(5)–C(5)	1.146(9)	O(6)–C(6)	1.147(9)
O(7)–C(7)	1.125(8)	O(8)–C(8)	1.117(9)
O(9)–C(9)	1.139(8)	O(10)–C(10)	1.124(9)
C(23)–C(24)	1.504(9)	C(23)–C(25)	1.329(8)
C(1)–Mo(1)–C(3)	88.2(3)	C(1)–Mo(1)–C(4)	92.2(3)
C(3)–Mo(1)–C(4)	87.5(3)	C(1)–Mo(1)–C(5)	90.6(3)
C(3)–Mo(1)–C(5)	173.5(3)	C(4)–Mo(1)–C(5)	86.1(3)
C(1)–Mo(1)–C(2)	88.5(3)	C(3)–Mo(1)–C(2)	90.7(3)
C(4)–Mo(1)–C(2)	178.1(3)	C(5)–Mo(1)–C(2)	95.6(3)
C(1)–Mo(1)–P(1)	173.1(2)	C(3)–Mo(1)–P(1)	95.8(2)
C(4)–Mo(1)–P(1)	93.5(2)	C(5)–Mo(1)–P(1)	86.0(2)
C(2)–Mo(1)–P(1)	85.9(2)	C(6)–Mo(2)–C(9)	90.6(3)
C(6)–Mo(2)–C(10)	87.6(3)	C(9)–Mo(2)–C(10)	90.5(3)
C(6)–Mo(2)–C(8)	89.6(3)	C(9)–Mo(2)–C(8)	87.3(3)
C(10)–Mo(2)–C(8)	176.4(3)	C(6)–Mo(2)–C(7)	91.5(3)
C(9)–Mo(2)–C(7)	175.4(3)	C(10)–Mo(2)–C(7)	93.7(3)
C(8)–Mo(2)–C(7)	88.6(3)	C(6)–Mo(2)–P(2)	179.1(2)
C(9)–Mo(2)–P(2)	89.6(2)	C(10)–Mo(2)–P(2)	93.2(2)
C(8)–Mo(2)–P(2)	89.6(2)	C(7)–Mo(2)–P(2)	88.2(2)
C(11)–P(1)–C(22)	90.1(4)	C(11)–P(1)–C(23)	101.6(3)
C(22)–P(1)–C(23)	102.7(3)	C(11)–P(1)–Mo(1)	115.0(2)
C(22)–P(1)–Mo(1)	120.0(2)	C(23)–P(1)–Mo(1)	121.7(2)
C(25)–P(2)–C(26)	102.3(3)	C(25)–P(2)–C(32)	103.2(3)
C(26)–P(2)–C(32)	103.0(3)	C(25)–P(2)–Mo(2)	114.9(2)
C(26)–P(2)–Mo(2)	120.3(2)	C(32)–P(2)–Mo(2)	111.1(2)
O(1)–C(1)–Mo(1)	179.3(7)	O(2)–C(2)–Mo(1)	177.2(7)
O(3)–C(3)–Mo(1)	176.7(7)	O(4)–C(4)–Mo(1)	177.7(8)
O(5)–C(5)–Mo(1)	177.2(7)	O(6)–C(6)–Mo(2)	178.2(8)
O(7)–C(7)–Mo(2)	176.1(7)	O(8)–C(8)–Mo(2)	177.5(8)
O(9)–C(9)–Mo(2)	178.3(7)	O(10)–C(10)–Mo(2)	177.0(7)
C(25)–C(23)–C(24)	124.5(6)	C(25)–C(23)–P(1)	118.7(5)
C(24)–C(23)–P(1)	116.8(5)	C(23)–C(25)–P(2)	126.0(5)

120(2)° (C20–C19–P2), indicate that C19 is sp^2 hybridized, and since the C19–C20 bond distance accounts for the presence of a carbon–carbon double bond, C20 is also sp^2 hybridized. In **4a** a distance of 1.55(2) Å for C18–C19 confirms the presence of a single bond. For all the chelate complexes the molybdenum–carbon bond lengths fall within the range of 2.016(4)–2.047(13) Å for Mo–C bonds *trans* to the carbon and within the range of 1.969(5)–1.999(4) Å for Mo–C bonds *trans* to the phosphorus. Here the σ-donor ability of the phosphine ligands toward the metal atoms is responsible for strengthening the *trans* metal–carbon bond by π-backbonding, which causes a shortening of the Mo–C bond distances. This in turn weakens the C–O bond due to the increased electron density in its π^* orbital. The bite angles (P–Mo–P) for the chelate complexes **5b**, **6a**, **6b** and **9** are 79.61(4)°, 77.55(3)°, 78.78(9)° and 83.57(3)° respectively and are in close agreement with reported literature values [13, 15, 16]. The reduced ring strain present for the six-membered ring when compared to the five-membered rings containing the constrained double bond may account for the higher P–Mo–P bond angle for **9**. The C17–C18 bond distances for complexes **5b**, **6a**, **6b** and **9** are 1.306(6), 1.328(4), 1.328(12) and 1.312(6) Å respectively, confirming the presence of double bonds in each case. Similarly the distances of 1.505(8) Å between C17 and C19 in **5b**, and 1.503(4) Å, 1.499(12) Å and 1.499(6) Å between C18 and C19 in **6a**, **6b** and **9** respectively, confirms the presence of single bonds. The molecular structure of complex **8** is shown in figure 8 and selected bond distances and angles are given in table VIII. The presence of the Mo_2P_2 core having a planar geometry is a typical characteristic for these types of compounds, and the metrical parameters are similar to those found for $Mo_2(CO)_8(\mu\text{-}PEt_2)_2$ [17]. The Mo–Mo bond distance of 3.047(3) Å signifies the presence of a single bond between the two metal atoms and is in close agreement with other reported values [17]. The metal–carbon bond distances for this bridged phosphide range between 1.95(3) and 2.00(3) Å, and the average values of the C–O bond lengths (1.16(2) Å) and the Mo–C–O bond angles (176(2)°) are in the normal ranges [17].

Table III. Selected bond lengths and angles for **4a**.

Mo(1)–C(4)	2.01(2)	Mo(1)–C(3)	2.01(3)
Mo(1)–C(5)	2.02(3)	Mo(1)–C(2)	2.03(3)
Mo(1)–C(1)	2.04(3)	Mo(1)–P(1)	2.502(5)
Mo(2)–C(37)	1.96(2)	Mo(2)–C(34)	2.00(2)
Mo(2)–C(36)	2.021(14)	Mo(2)–C(35)	2.03(2)
Mo(2)–C(33)	2.06(2)	Mo(2)–P(2)	2.527(5)
P(1)–C(17)	1.77(2)	P(1)–C(6)	1.82(2)
P(1)–C(18)	1.86(2)	P(2)–C(19)	1.79(2)
P(2)–C(21)	1.83(2)	P(2)–C(27)	1.83(2)
O(1)–C(1)	1.09(2)	O(2)–C(2)	1.12(2)
O(3)–C(3)	1.14(2)	O(4)–C(4)	1.13(2)
O(5)–C(5)	1.13(3)	O(6)–C(33)	1.06(2)
O(7)–C(34)	1.03(2)	O(8)–C(35)	1.04(2)
O(9)–C(36)	1.04(2)	O(10)–C(37)	1.04(2)
C(19)–C(20)	1.31(2)	C(18)–C(19)	1.55(2)
C(4)–Mo(1)–C(3)	88.8(9)	C(4)–Mo(1)–C(5)	92.1(9)
C(3)–Mo(1)–C(5)	178.5(10)	C(4)–Mo(1)–C(2)	176.2(9)
C(3)–Mo(1)–C(2)	87.5(9)	C(5)–Mo(1)–C(2)	91.6(10)
C(4)–Mo(1)–C(1)	88.4(8)	C(3)–Mo(1)–C(1)	89.9(9)
C(5)–Mo(1)–C(1)	88.9(10)	C(2)–Mo(1)–C(1)	90.5(9)
C(4)–Mo(1)–P(1)	91.4(6)	C(3)–Mo(1)–P(1)	90.2(6)
C(5)–Mo(1)–P(1)	91.0(7)	C(2)–Mo(1)–P(1)	89.7(7)
C(1)–Mo(1)–P(1)	179.8(7)	C(37)–Mo(2)–C(34)	91.3(5)
C(37)–Mo(2)–C(36)	90.7(5)	C(34)–Mo(2)–C(36)	175.3(13)
C(37)–Mo(2)–C(35)	177.1(13)	C(34)–Mo(2)–C(35)	89.2(5)
C(36)–Mo(2)–C(35)	88.5(5)	C(37)–Mo(2)–C(33)	89.6(8)
C(34)–Mo(2)–C(33)	88.4(8)	C(36)–Mo(2)–C(33)	87.4(7)
C(35)–Mo(2)–C(33)	87.6(8)	C(37)–Mo(2)–P(2)	88.1(11)
C(34)–Mo(2)–P(2)	97.7(10)	C(36)–Mo(2)–P(2)	86.5(10)
C(35)–Mo(2)–P(2)	94.7(10)	C(33)–Mo(2)–P(2)	173.5(8)
C(17)–P(1)–C(6)	90.9(9)	C(17)–P(1)–C(18)	107.2(9)
C(6)–P(1)–C(18)	106.9(8)	C(17)–P(1)–Mo(1)	118.6(6)
C(6)–P(1)–Mo(1)	118.7(6)	C(18)–P(1)–Mo(1)	112.2(6)
C(19)–P(2)–C(21)	101.7(9)	C(19)–P(2)–C(27)	104.0(9)
C(21)–P(2)–C(27)	103.9(9)	C(19)–P(2)–Mo(2)	118.9(7)
C(21)–P(2)–Mo(2)	119.2(6)	C(27)–P(2)–Mo(2)	107.3(6)
O(1)–C(1)–Mo(1)	178(2)	O(2)–C(2)–Mo(1)	176(2)
O(3)–C(3)–Mo(1)	179(2)	O(4)–C(4)–Mo(1)	178(2)
O(5)–C(5)–Mo(1)	176(2)	C(7)–C(6)–C(11)	122(2)
C(7)–C(6)–P(1)	128(2)	C(19)–C(18)–P(1)	122.5(12)
C(20)–C(19)–C(18)	122(2)	C(20)–C(19)–P(2)	120(2)
C(18)–C(19)–P(2)	117.9(14)	O(6)–C(33)–Mo(2)	176(3)
O(7)–C(34)–Mo(2)	174(3)	O(8)–C(35)–Mo(2)	176(3)
O(9)–C(36)–Mo(2)	174(3)	O(10)–C(37)–Mo(2)	175(3)

Experimental section

Reagents and physical measurements

Commercially available reagent grade chemicals were used unless otherwise indicated. All experiments were performed under a dry nitrogen atmosphere using standard Schlenk-line techniques. $(RPh_2P)Mo(CO)_5$ and $(RDBP)Mo(CO)_5$ where R = H, $CH_2C{\equiv}CH$, were prepared by literature methods [8]. Tetrahydrofuran was distilled under nitrogen from sodium benzophenoneketyl, and diglyme was distilled under nitrogen over sodium. Silica gel for column chromatography (grade 12, 28–200 mesh) was obtained from Aldrich. Melting points were determined on a Mel-Temp apparatus and are uncorrected. Elemental analyses were performed by Galibraith Laboratories, Knoxville, TN. Solution infrared spectra were obtained on a Perkin-Elmer Paragon 1000 PC FT spectrometer in sealed CaF_2 cells. $^{31}P\{^1H\}$, $^{13}C\{^1H\}$ and ^1H NMR spectra were recorded at 121.66 (202.35), 75 (125.71) and 300 (499.86) MHz, respectively, on either a General Electric GN-300 or Varian Unity Plus-500

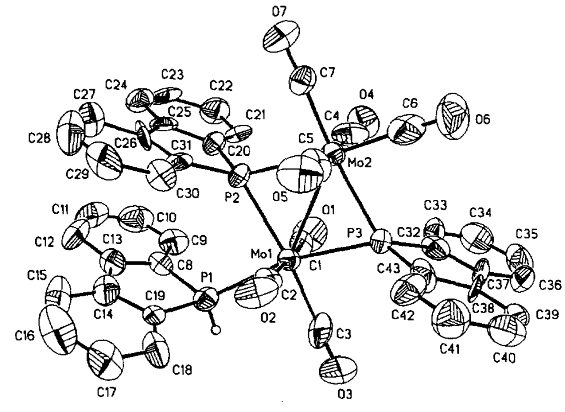

Fig 8. Structural drawing of **8** showing the atom numbering scheme (40% probability ellipsoids). All hydrogen atoms have been omitted for clarity except on P1 which has an arbitrary radius of 0.1 Å.

Table IV. Selected bond lengths and angles for **5b**.

Mo–C(2)	1.969(5)	Mo–C(1)	1.992(5)
Mo–C(4)	2.025(5)	Mo–C(3)	2.037(5)
Mo–P(1)	2.4847(12)	Mo–P(2)	2.5306(11)
P(1)–C(5)	1.809(4)	P(1)–C(16)	1.823(4)
P(1)–C(17)	1.837(4)	P(2)–C(26)	1.822(4)
P(2)–C(20)	1.831(5)	P(2)–C(19)	1.846(4)
O(1)–C(1)	1.148(5)	O(2)–C(2)	1.150(5)
O(3)–C(3)	1.138(5)	O(4)–C(4)	1.144(5)
C(17)–C(19)	1.506(6)	C(17)–C(18)	1.306(6)
C(2)–Mo–C(1)	89.6(2)	C(2)–Mo–C(4)	87.9(2)
C(1)–Mo–C(4)	91.6(2)	C(2)–Mo–C(3)	87.4(2)
C(1)–Mo–C(3)	90.8(2)	C(4)–Mo–C(3)	174.7(2)
C(2)–Mo–P(1)	96.7(2)	C(1)–Mo–P(1)	173.35(14)
C(4)–Mo–P(1)	90.77(12)	C(3)–Mo–P(1)	87.40(13)
C(2)–Mo–P(2)	176.3(2)	C(1)–Mo–P(2)	94.06(14)
C(4)–Mo–P(2)	92.31(13)	C(3)–Mo–P(2)	92.30(14)
P(1)–Mo–P(2)	79.61(4)	C(5)–P(1)–C(16)	90.4(2)
C(5)–P(1)–C(17)	105.0(2)	C(16)–P(1)–C(17)	103.4(2)
C(5)–P(1)–Mo	128.5(2)	C(16)–P(1)–Mo	122.65(14)
C(17)–P(1)–Mo	103.75(13)	C(26)–P(2)–C(20)	101.8(2)
C(26)–P(2)–C(19)	103.0(2)	C(20)–P(2)–C(19)	103.7(2)
C(26)–P(2)–Mo	119.37(14)	C(20)–P(2)–Mo	118.5(2)
C(19)–P(2)–Mo	108.38(14)	O(1)–C(1)–Mo	178.6(4)
O(2)–C(2)–Mo	178.4(5)	O(3)–C(3)–Mo	175.9(4)
O(4)–C(4)–Mo	176.8(4)	C(18)–C(17)–C(19)	124.5(4)
C(18)–C(17)–P(1)	124.4(4)	C(19)–C(17)–P(1)	110.6(3)
C(17)–C(19)–P(2)	109.6(3)		

Table V. Selected bond lengths and angles for **6a**.

Mo(1)–C(3)	1.991(4)	Mo(1)–C(4)	1.991(4)
Mo(1)–C(1)	2.032(4)	Mo(1)–C(2)	2.040(4)
Mo(1)–P(1)	2.4845(9)	Mo(1)–P(2)	2.4946(9)
P(1)–C(5)	1.818(3)	P(1)–C(17)	1.819(3)
P(1)–C(16)	1.820(3)	P(2)–C(26)	1.830(3)
P(2)–C(20)	1.836(3)	P(2)–C(18)	1.841(3)
O(1)–C(1)	1.135(4)	O(2)–C(2)	1.138(4)
O(3)–C(3)	1.150(4)	O(4)–C(4)	1.149(4)
C(18)–C(19)	1.503(4)	C(17)–C(18)	1.328(4)
C(3)–Mo(1)–C(4)	89.09(14)	C(3)–Mo(1)–C(1)	94.37(14)
C(4)–Mo(1)–C(1)	87.53(13)	C(3)–Mo(1)–C(2)	89.09(14)
C(4)–Mo(1)–C(2)	89.67(13)	C(1)–Mo(1)–C(2)	175.51(14)
C(3)–Mo(1)–P(1)	170.23(10)	C(4)–Mo(1)–P(1)	100.68(10)
C(1)–Mo(1)–P(1)	86.01(9)	C(2)–Mo(1)–P(1)	91.06(10)
C(3)–Mo(1)–P(2)	92.69(10)	C(4)–Mo(1)–P(2)	176.45(10)
C(1)–Mo(1)–P(2)	89.27(9)	C(2)–Mo(1)–P(2)	93.43(10)
P(1)–Mo(1)–P(2)	77.55(3)	C(5)–P(1)–C(17)	102.8(2)
C(5)–P(1)–C(16)	90.3(2)	C(17)–P(1)–C(16)	106.6(2)
C(5)–P(1)–Mo(1)	126.15(11)	C(17)–P(1)–Mo(1)	107.96(11)
C(16)–P(1)–Mo(1)	120.29(11)	C(26)–P(2)–C(20)	102.4(2)
C(26)–P(2)–C(18)	101.98(14)	C(20)–P(2)–C(18)	104.6(2)
C(26)–P(2)–Mo(1)	117.39(11)	C(20)–P(2)–Mo(1)	119.67(12)
C(18)–P(2)–Mo(1)	108.77(11)	O(1)–C(1)–Mo(1)	177.9(3)
O(2)–C(2)–Mo(1)	177.7(3)	O(3)–C(3)–Mo(1)	179.4(3)
O(4)–C(4)–Mo(1)	176.2(3)	C(6)–C(5)–C(10)	120.5(3)
C(18)–C(17)–P(1)	122.2(3)	C(17)–C(18)–C(19)	123.3(3)
C(17)–C(18)–P(2)	116.2(2)	C(19)–C(18)–P(2)	120.4(2)

spectrometer. Proton and carbon chemical shifts are relative to internal Me_4Si, phosphorus chemical shifts are relative to external PPh_3 ($\delta^{31}P = -6.0$ ppm); all shifts to low field (high frequency) are positive.

• *Base-catalyzed reaction of* **1a** *with* **2b**

(i) To a solution of 2.00 g (4.74 mmol) of **1a** in 20 mL of freshly distilled dry THF was added a catalytic amount of $KOBu^t$ ($\sim$ 0.01 g), and the mixture was stirred under nitrogen for 5–6 min. The solution turned bright orange red. To this mixture was added a solution of 2.17 g (4.74 mmol) of **2b** in 20 mL of dry THF. The total volume of the reaction mixture was increased to 200 mL by adding excess dry THF, and the mixture was refluxed for 24 h under nitrogen. The resulting solution was reddish brown in color. After cooling to room temperature, 50 mL of hexane and 50 mL of diethyl ether were added to the product mixture

Table VI. Selected bond lengths and angles for **6b**.

Mo(1)-C(4)	1.979(13)	Mo(1)-C(3)	1.994(12)
Mo(1)-C(2)	2.015(13)	Mo(1)-C(1)	2.047(13)
Mo(1)-P(1)	2.475(3)	Mo(1)-P(2)	2.487(3)
P(2)-C(17)	1.791(10)	P(2)-C(11)	1.825(12)
P(2)-C(5)	1.852(11)	P(1)-C(20)	1.826(10)
P(1)-C(31)	1.828(11)	P(1)-C(18)	1.842(10)
O(1)-C(1)	1.120(12)	O(2)-C(2)	1.142(12)
O(3)-C(3)	1.142(11)	O(4)-C(4)	1.164(12)
C(17)-C(18)	1.328(12)	C(18)-C(19)	1.499(12)
C(4)-Mo(1)-C(3)	94.3(5)	C(4)-Mo(1)-C(2)	90.5(5)
C(3)-Mo(1)-C(2)	85.8(4)	C(4)-Mo(1)-C(1)	87.4(5)
C(3)-Mo(1)-C(1)	89.4(4)	C(2)-Mo(1)-C(1)	174.6(4)
C(4)-Mo(1)-P(1)	93.6(3)	C(3)-Mo(1)-P(1)	171.8(4)
C(2)-Mo(1)-P(1)	91.8(3)	C(1)-Mo(1)-P(1)	93.4(3)
C(4)-Mo(1)-P(2)	172.4(3)	C(3)-Mo(1)-P(2)	93.3(4)
C(2)-Mo(1)-P(2)	89.5(3)	C(1)-Mo(1)-P(2)	93.2(3)
P(1)-Mo(1)-P(2)	78.78(9)	C(17)-P(2)-C(11)	105.3(5)
C(17)-P(2)-C(5)	99.8(5)	C(11)-P(2)-C(5)	102.2(5)
C(17)-P(2)-Mo(1)	109.0(4)	C(11)-P(2)-Mo(1)	118.3(4)
C(5)-P(2)-Mo(1)	119.9(3)	C(20)-P(1)-C(31)	90.5(5)
C(20)-P(1)-C(18)	100.7(5)	C(31)-P(1)-C(18)	103.2(5)
C(20)-P(1)-Mo(1)	125.0(4)	C(31)-P(1)-Mo(1)	122.4(3)
C(18)-P(1)-Mo(1)	110.9(3)	O(1)-C(1)-Mo(1)	173.5(12)
O(2)-C(2)-Mo(1)	176.6(11)	O(3)-C(3)-Mo(1)	178.6(12)
O(4)-C(4)-Mo(1)	179.3(10)	C(18)-C(17)-P(2)	124.2(9)
C(17)-C(18)-C(19)	125.2(10)	C(17)-C(18)-P(1)	116.0(8)
C(19)-C(18)-P(1)	118.7(8)		

Table VII. Selected bond lengths and angles for **9**.

Mo-C(2)	1.986(4)	Mo-C(1)	1.999(4)
Mo-C(4)	2.016(4)	Mo-C(3)	2.041(5)
Mo-P(1)	2.4718(10)	Mo-P(2)	2.5100(10)
P(1)-C(17)	1.814(4)	P(1)-C(16)	1.820(4)
P(1)-C(5)	1.826(4)	P(2)-C(20)	1.828(4)
P(2)-C(26)	1.833(4)	P(2)-C(19)	1.845(4)
O(1)-C(1)	1.145(5)	O(2)-C(2)	1.150(5)
O(3)-C(3)	1.145(5)	O(4)-C(4)	1.149(5)
C(18)-C(19)	1.499(6)	C(17)-C(18)	1.312(6)
C(2)-Mo-C(1)	90.4(2)	C(2)-Mo-C(4)	88.5(2)
C(1)-Mo-C(4)	89.4(2)	C(2)-Mo-C(3)	84.4(2)
C(1)-Mo-C(3)	90.6(2)	C(4)-Mo-C(3)	172.9(2)
C(2)-Mo-P(1)	90.82(12)	C(1)-Mo-P(1)	178.28(11)
C(4)-Mo-P(1)	89.40(11)	C(3)-Mo-P(1)	90.79(11)
C(2)-Mo-P(2)	174.39(12)	C(1)-Mo-P(2)	95.23(11)
C(4)-Mo-P(2)	91.44(11)	C(3)-Mo-P(2)	95.64(11)
P(1)-Mo-P(2)	83.57(3)	C(17)-P(1)-C(16)	102.0(2)
C(17)-P(1)-C(5)	101.0(2)	C(16)-P(1)-C(5)	90.2(2)
C(17)-P(1)-Mo	120.47(13)	C(16)-P(1)-Mo	119.35(12)
C(5)-P(1)-Mo	118.29(12)	C(20)-P(2)-C(26)	103.0(2)
C(20)-P(2)-C(19)	103.0(2)	C(26)-P(2)-C(19)	99.6(2)
C(20)-P(2)-Mo	117.26(12)	C(26)-P(2)-Mo	120.44(12)
C(19)-P(2)-Mo	110.79(13)	O(1)-C(1)-Mo	176.6(3)
O(2)-C(2)-Mo	178.2(4)	O(3)-C(3)-Mo	174.6(3)
O(4)-C(4)-Mo	175.6(3)	C(18)-C(17)-P(1)	128.2(3)
C(17)-C(18)-C(19)	130.5(4)	C(18)-C(19)-P(2)	117.4(3)

which was washed with three 100 mL portions of 1.0 M HCl and three 100 mL portions of water. The organic layer was dried with $MgSO_4$ and gravity filtered. The solvent from the filtrate was removed on a rotary evaporator, and the resulting mixture of compounds was separated by column chromatography on silica gel using a solution of 5% benzene in hexane as the eluent. The amount of benzene in the eluent was gradually increased. Twenty four fractions of 50–75 mL each were collected and were monitored by TLC and $^{31}P\{^1H\}$ NMR spectroscopy. From the first four fractions about 0.375 g of unreacted starting material **1a** and diphenylphosphine oxide was retrieved. Fractions 5–6 gave 0.36 g (0.41 mmol, 8.7%) of complex **3a**. Upon changing the concentration of the eluent to 10% benzene in hexane about 0.27 g of material was recovered from fractions 7–8 which contained 0.15 g (0.191 mmol, 8.1%) of complex **7** that was precipitated out as a red solid by repeated fractional crystallization from a mixed solvent system of methylene chlo-

Table VIII. Selected bond lengths and angles for **8**.

Mo(1)–C(2)	1.98(2)	Mo(1)–C(3)	1.98(3)
Mo(1)–C(1)	1.99(2)	Mo(1)–P(3)	2.427(6)
Mo(1)–P(2)	2.467(6)	Mo(1)–P(1)	2.490(6)
Mo(1)–Mo(2)	3.047(3)	Mo(2)–C(6)	1.95(3)
Mo(2)–C(7)	1.95(2)	Mo(2)–C(4)	1.98(3)
Mo(2)–C(5)	2.00(3)	Mo(2)–P(3)	2.487(6)
Mo(2)–P(2)	2.514(6)	P(1)–C(19)	1.74(2)
P(1)–C(8)	1.83(2)	P(2)–C(31)	1.76(2)
P(2)–C(20)	1.79(2)	P(3)–C(32)	1.79(2)
P(3)–C(43)	1.81(3)	O(1)–C(1)	1.17(2)
O(2)–C(2)	1.17(2)	O(3)–C(3)	1.14(2)
O(4)–C(4)	1.15(2)	O(5)–C(5)	1.16(2)
O(6)–C(6)	1.16(3)	O(7)–C(7)	1.17(2)
C(2)–Mo(1)–C(3)	90.5(10)	C(2)–Mo(1)–C(1)	175.5(8)
C(3)–Mo(1)–C(1)	90.1(10)	C(2)–Mo(1)–P(3)	90.7(6)
C(3)–Mo(1)–P(3)	81.3(8)	C(1)–Mo(1)–P(3)	93.8(6)
C(2)–Mo(1)–P(2)	89.3(6)	C(3)–Mo(1)–P(2)	173.2(7)
C(1)–Mo(1)–P(2)	89.5(6)	P(3)–Mo(1)–P(2)	105.5(2)
C(2)–Mo(1)–P(1)	87.7(5)	C(3)–Mo(1)–P(1)	85.5(7)
C(1)–Mo(1)–P(1)	87.9(6)	P(3)–Mo(1)–P(1)	166.7(2)
P(2)–Mo(1)–P(1)	87.7(2)	C(2)–Mo(1)–Mo(2)	87.7(5)
C(3)–Mo(1)–Mo(2)	133.8(8)	C(1)–Mo(1)–Mo(2)	95.1(6)
P(3)–Mo(1)–Mo(2)	52.6(2)	P(2)–Mo(1)–Mo(2)	52.97(14)
P(1)–Mo(1)–Mo(2)	140.5(2)	C(6)–Mo(2)–C(7)	90.7(10)
C(6)–Mo(2)–C(4)	88.6(12)	C(7)–Mo(2)–C(4)	87.9(10)
C(6)–Mo(2)–C(5)	87.8(11)	C(7)–Mo(2)–C(5)	86.0(10)
C(4)–Mo(2)–C(5)	172.8(10)	C(6)–Mo(2)–P(3)	82.9(7)
C(7)–Mo(2)–P(3)	173.6(6)	C(4)–Mo(2)–P(3)	91.3(7)
C(5)–Mo(2)–P(3)	94.4(7)	C(6)–Mo(2)–P(2)	174.7(8)
C(7)–Mo(2)–P(2)	84.1(6)	C(4)–Mo(2)–P(2)	90.3(8)
C(5)–Mo(2)–P(2)	92.8(7)	P(3)–Mo(2)–P(2)	102.3(2)
C(6)–Mo(2)–Mo(1)	133.7(7)	C(7)–Mo(2)–Mo(1)	135.6(6)
C(4)–Mo(2)–Mo(1)	93.6(7)	C(5)–Mo(2)–Mo(1)	93.5(7)
P(3)–Mo(2)–Mo(1)	50.79(14)	P(2)–Mo(2)–Mo(1)	51.58(14)
C(19)–P(1)–C(8)	89.9(12)	C(19)–P(1)–Mo(1)	119.9(8)
C(8)–P(1)–Mo(1)	122.8(7)	C(31)–P(2)–C(20)	91.2(11)
C(31)–P(2)–Mo(1)	126.3(8)	C(20)–P(2)–Mo(1)	124.6(7)
C(31)–P(2)–Mo(2)	122.2(7)	C(20)–P(2)–Mo(2)	121.1(8)
Mo(1)–P(2)–Mo(2)	75.4(2)	C(32)–P(3)–C(43)	89.0(14)
C(32)–P(3)–Mo(1)	126.1(10)	C(43)–P(3)–Mo(1)	125.6(9)
C(32)–P(3)–Mo(2)	123.3(9)	C(43)–P(3)–Mo(2)	120.9(9)
Mo(1)–P(3)–Mo(2)	76.6(2)	O(1)–C(1)–Mo(1)	178(2)
O(2)–C(2)–Mo(1)	178(2)	O(3)–C(3)–Mo(1)	174(3)
O(4)–C(4)–Mo(2)	174(3)	O(5)–C(5)–Mo(2)	177(2)
O(6)–C(6)–Mo(2)	177(2)	O(7)–C(7)–Mo(2)	177(2)

ride and methanol. The residue contained **3a**, **4a** and other impurities which could not be further separated. The column was then eluted with 15% benzene in hexane solution. Fractions 9–10 eluted 0.15 g of material which was comprised of **4a** and at least four other compounds that could not be separated for complete characterization. Attempts to separate these products by fractional crystallization from a mixed solvent system of methylene chloride, ether and methanol caused **4a** to crystallize out as large yellow-green prolate spheroid crystals along with the co-precipitation of an amorphous yellowish solid, the latter being the aforementioned impurities. We were able to hand-pick a few of these prolate spheroid crystals to complete the spectral characterization for complex **4a**. Upon changing the eluent to 20% benzene in hexane, fractions 10–11 eluted trace amounts of complex **4a** which could not be recovered. The eluent was then gradually changed to 75% benzene in hexane. About 1.48 g (2.40 mmol, 50.6%) of **5a** was eluted last from the column in fractions 14–24. It was crystallized from a 1:1:1 mixture of methylene chloride, ether and methanol to give pale yellow crystals.

(ii) The same reaction was repeated in diglyme but the crude product mixture was only characterized by $^{31}P\{^{1}H\}$ NMR spectroscopy (table IX).

- *Base-catalyzed reaction of* ***1b*** *with* ***2a***

(i) To a solution of 2.08 g (4.52 mmol) of **2a** in 80 mL of freshly distilled THF was added 1.90 g (4.52 mmol) of **1b** under a nitrogen atmosphere, and the mixture was stirred for 10 min. A catalytic amount of $KOBu^t$ (~0.01 g) was then added, and the reaction mixture was refluxed under nitrogen for 8 h. The color of the solution remained bright yellow orange. The mixture was cooled to ambient temperature, and then 50 mL of hexane and 50 mL of diethyl ether were added. The organic phase was washed with three 75 mL portions of 1.0 M HCl and two 100 mL portions of water followed by drying with $MgSO_4$. The solvent was removed on a rotary evaporator, and the resulting mixture of products was separated by column chromatography on silica gel using 5% benzene in hexane solution as the eluent. The benzene concentration of the solution was gradually increased. Thirty-one fractions of 50–75 mL were collected and were monitored by TLC and $^{31}P\{^1H\}$ NMR spectroscopy. Approximately 0.36 g of **1b** and dibenzophosphole oxide were collected from fractions 5–9 and 0.59 g (1.28 mmol) of **2a** and its isomer **2a″** was recovered from fraction 10. Fractions 11–15 gave 0.85 g (0.96 mmol, 29.6%) of complex **3b**. Upon increasing to 10% benzene in hexane, a mixture of **3b**, **4b** and trace amounts of impurities were eluted in fractions 16–18 (see above). We were unable to separate **4b** from this mixture to completely characterize it. Complex **5b** (0.28 g, 0.45 mmol, 14.0%) was eluted next in fractions 20–22 when the eluent was increased to 20% benzene in hexane. Fractions 24–26 came out as a deep reddish brown band on the column when eluted with 25% benzene in hexane solution and crystallized to give 0.005 g (0.0053 mmol) of complex **8**. Upon increasing to 50% benzene in hexane, 0.09 g (0.146 mmol, 4.5%) of complex **9** was eluted last from the column in fractions 28–31. All the above-mentioned complexes were recrystallized from a 1:1:1 mixture of methylene chloride / ether / methanol.

(ii) To a solution containing 2.00 g (4.35 mmol) of **2a** and 1.83 g (4.35 mmol) of **1b** in 75 mL of freshly distilled diglyme with stirring under nitrogen was added a catalytic amount of KOBu^t ($\sim$0.02 g) and the mixture was refluxed for 8 h. Colorless crystals of $Mo(CO)_6$ formed on the inside of the reflux condenser. After cooling to ambient temperature, the solvent was removed by vacuum distillation while keeping the flask warm in a hot water bath. The yellowish brown residue was dissolved in 150 mL of diethyl ether and 50 mL hexane and washed with 3 × 100 mL portions of 1.0 M HCl and 3 × 100 mL portions of water followed by drying with $MgSO_4$. The solvents were removed by rotary evaporation. The crude products were separated by column chromatography on silica gel with 5% benzene in hexane solution as the eluent. Thirty four fractions of 50–75 mL each were collected and monitored by TLC and $^{31}P\{^1H\}$ NMR spectroscopy. About 0.02 g of unreacted **1b** and dibenzophosphole oxide were recovered from fractions 1–4 and 0.25 g (0.54 mmol) of unreacted **2a** and its isomer **2a″** were recovered from fractions 6–10. Fractions 11–12 gave about 0.1 g of **3b** contaminated with some **2a**. Fractions 13–15 gave about 0.85 g (0.97 mmol,25.4%) of complex **3b**. The benzene concentration of the eluent was gradually increased to 15% benzene in hexane when 0.085 g (0.14 mmol, 0.73%) of complex **10** was eluted from fractions 19–22. Complex **5b** (0.89 g, 1.45 mmol, 38.1%) was eluted next in fractions 23–26 when the eluent concentration was changed to 20% benzene in hexane solution. It was contaminated with trace amounts of **6b** in fraction 26. The former fractions of this batch (23–24) were contaminated with trace amounts of another unknown complex of which the $^{31}P\{^1H\}$ NMR spectrum showed resonances at δ 190.1 (d, J_{PP} = 36.35 Hz), d 166.3 (d, J_{PP} = 30.55 Hz) and d 19.12 (dd, J_{PP} = 36.35 Hz and 30.55 Hz) respectively, indicating the presence of three inequivalent phosphorus nuclei in the molecule. Lastly, 0.45 g (0.73 mmol, 19.2%) of complex **9** was eluted from the column in fractions 28–32 when the eluent was increased to $\sim$50% benzene in hexane. All the above-mentioned complexes obtained from the different fractions were recrystallized from a 1:1:1 mixture of methylene chloride / ether / methanol.

- *Base-catalyzed isomerization of* **5a**

To a solution of 0.60 g (0.98 mmol) of **5a** in 100 mL of freshly distilled diglyme was added a catalytic amount of KOBu^t ($\sim$0.005 g), and the reaction mixture was refluxed for 24 h with stirring under a nitrogen atmosphere. The contents of the flask were cooled to ambient temperature, and the solvent was removed by vacuum distillation by keeping the flask warm with a hot water bath. The residue was dissolved in 100 mL of methylene chloride and was washed with 2 × 100 mL portions of 1.0 M HCl solution followed by 2 × 100 mL portions of distilled water. The organic phase was then dried with $MgSO_4$, and the volume of the solvent was reduced to $\sim$15 mL by rotary evaporation. To this was added an equal volume of ether and methanol and it was allowed to stand for 24 h at −20 °C, whereby 0.54 g (0.88 mmol, 90.2%) of pale yellow crystals of complex **6a** separated out.

- *Base-catalyzed isomerization of* **5b**

A catalytic amount of KOBu^t ($\sim$0.005 g) was added to a solution of 0.41 g (0.66 mmol) of **5b** in 100 mL of freshly distilled diglyme. The solution was refluxed for 4 h and then stirred at room temperature overnight under a nitrogen atmosphere. The reaction flask was kept warm on a hot water bath as the solvent was removed by vacuum distillation. Work-up and crystallization of the reaction mixture as mentioned above gave 0.35 g (0.57 mmol, 86.2%) of pale yellow crystals of complex **6b**.

The ratios of the products formed as determined by $^{31}P\{^1H\}$ NMR spectroscopy of the crude reaction mixture after workup but prior to chromatography are given in table IX.

Table IX. Ratios of products as determined by $^{31}P\{^1H\}$ NMR spectroscopy of the crude product mixtures dissolved in $CDCl_3$.

Reactants	(solvent)	Ratios of Products						
		3a	**4a**	**5a**	**7**			
1a + **2b**	(THF)	1.0	1.3	2.1	ND[a]			
1a + **2b**	(Diglyme)	ND	1.0	1.7	0.3			
		3b	**4b**	**5b**	**6b**	**8**	**9**	**10**
1b + **2a**	(THF)	4.2	1.9	2.6	ND	ND	ND	1.0
1b + **2a**	(Diglyme)	4.7	ND	21.0	5.4	1.0	1.6	4.7

[a] ND: not detected; less than 5% of total phosphorus species.

Characterization of the complexes

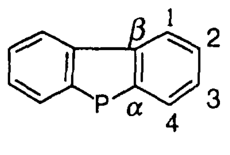

3a: Pale yellow solid.

Mp: > 154 °C (dec).

IR (CH_2Cl_2): ν_{CO} (cm^{-1}) 2 073 (m), 2 064 (sh), 1 990 (sh), 1 951 (s).

^1H NMR ($CDCl_3$, 500 MHz) δ 1.54 (ddd, $^3J_{PH}$ = 11.5 Hz, $^4J_{PH}$ = $^4J_{HH}$ = 1.0 Hz, 3H, CH_3), 6.52 (ddq, $^3J_{PH}$ = 31.0 Hz, $^2J_{PH}$ = 19.0 Hz, $^4J_{HH}$ = 1.0 Hz, 1H, C=C*H*), 7.32–7.94 (m, 18H, aromatic H's).

$^{13}C\{^1H\}$ NMR ($CDCl_3$, 125.71 MHz) δ 18.66 (dd, $^2J_{PC}$ = 13.7 Hz, $^3J_{PC}$ = 8.8 Hz, CH_3), 121.85 (d, $^3J_{PC}$ = 5.15 Hz, C_1), 128.85 (d, $^3J_{PC}$ = 9.43 Hz, C_m, C_3), 130.07 (d, $^2J_{PC}$ = 15.21 Hz, C_4), 130.75 (dd, $^1J_{PC}$ = 40.06 Hz, $^4J_{PC}$ = 1.70 Hz, C_i), 132.47 (s, C_2/C_P), 132.74 (s, C_2/C_P), 132.86 (d, $^2J_{PC}$ = 12.31 Hz, C_o), 134.59 (dd, $^1J_{PC}$ = 13.58 Hz, $^2J_{PC}$ = 10.43 Hz, $CH_3C{=}\mathit{C}H$), 138.49 (d, $^1J_{PC}$ = 42.49 Hz, C_α), 141.62 (d, $^2J_{PC}$ = 8.67 Hz, C_β), 150.16 (dd, $^1J_{PC}$ = 17.47 Hz, $^2J_{PC}$ = 7.17 Hz, $CH_3\mathit{C}{=}CH$), 204.69 (d, $^2J_{PC}$ = 8.92 Hz, 4CO, *cis*), 205.29 (d, $^2J_{PC}$ = 8.67 Hz, 4CO′, *cis*), 209.05 (d, $^2J_{PC}$ = 21.87 Hz, CO, *trans*), 209.57 (d, $^2J_{PC}$ = 23.26 Hz, CO′, *trans*).

$^{31}\mathrm{P}\{^{1}\mathrm{H}\}$ NMR ($\mathrm{CDCl_3}$, 121.66 MHz) δ 18.1 (d, $^{3}J_{\mathrm{PP}} = 22.5$ Hz, $\mathrm{P_A}$), 53.0 (d, $^{3}J_{\mathrm{PP}} = 22.5$ Hz, $\mathrm{P_x}$).

Anal Calc for $\mathrm{C_{37}H_{22}Mo_2O_{10}P_2}$: C, 50.48; H, 2.52. Found: C, 50.37; H, 2.61.

3b: Pale yellow solid.

Mp: > 166 °C (dec).

IR ($\mathrm{CH_2Cl_2}$): ν_{CO} ($\mathrm{cm^{-1}}$) 2 074 (m), 2 066 (sh), 1 990 (sh), 1 951 (s).

^{1}H NMR ($\mathrm{CDCl_3}$, 500 MHz) δ 1.17 (d, $^{3}J_{\mathrm{PH}} = 10$ Hz, 3H, $\mathrm{CH_3}$), 7.35–7.95 (m, 19H, $\mathrm{C{=}C}H$ and aromatic H′s).

$^{13}\mathrm{C}\{^{1}\mathrm{H}\}$ NMR ($\mathrm{CDCl_3}$, 125.71 MHz) δ 17.48 (dd, $^{2}J_{\mathrm{PC}} = 9.12$ Hz, $^{3}J_{\mathrm{PC}} = 6.98$ Hz, $\mathrm{CH_3}$), 121.78 (d, $^{3}J_{\mathrm{PC}} = 4.78$ Hz, $\mathrm{C_1}$), 128.73 (d, $^{3}J_{\mathrm{PC}} = 10.18$ Hz, $\mathrm{C_3}$), 128.92 (d, $^{3}J_{\mathrm{PC}} = 9.55$ Hz, $\mathrm{C_m}$), 130.08 (d, $^{2}J_{\mathrm{PC}} = 15.46$ Hz, $\mathrm{C_4}$), 130.2 (s, $\mathrm{C_2/C_P}$), 131.07 (s, $\mathrm{C_2/C_P}$), 131.86 (d, $^{2}J_{\mathrm{PC}} = 12.32$ Hz, $\mathrm{C_o}$), 135.44 (d, $^{1}J_{\mathrm{PC}} = 37.33$ Hz, $\mathrm{C_i}$), 138.27 (d, $^{1}J_{\mathrm{PC}} = 40.60$ Hz, $\mathrm{C_\alpha}$), 141.62 (dd, $^{1}J_{\mathrm{PC}} = {}^{2}J_{\mathrm{PC}} = 22.94$ Hz, $\mathrm{CH_3C{=}}C\mathrm{H}$), 142.18 (d, $^{2}J_{\mathrm{PC}} = 6.91$ Hz, $\mathrm{C_\beta}$), 147.36 (dd, $^{1}J_{\mathrm{PC}} = 15.78$ Hz, $^{2}J_{\mathrm{PC}} = 2.96$ Hz, $\mathrm{CH_3}C\mathrm{{=}CH}$), 204.9 (d, $^{2}J_{\mathrm{PC}} = 8.55$ Hz, 4CO, *cis*), 205.14 (d, $^{2}J_{\mathrm{PC}} = 9.55$ Hz, 4CO′, *cis*), 208.63 (d, $^{2}J_{\mathrm{PC}} = 22.88$ Hz, CO, *trans*), 209.70 (d, $^{2}J_{\mathrm{PC}} = 22.50$ Hz, CO′, *trans*).

$^{31}\mathrm{P}\{^{1}\mathrm{H}\}$ NMR ($\mathrm{CDCl_3}$, 121.66 MHz) δ 24.87 (d, $^{3}J_{\mathrm{PP}} = 33.21$ Hz, $\mathrm{P_A}$), 45.96 (d, $^{3}J_{\mathrm{PP}} = 33.21$ Hz, $\mathrm{P_x}$).

Anal Calc for $\mathrm{C_{37}H_{22}Mo_2O_{10}P_2}$: C, 50.48; H, 2.52. Found: C, 50.51; H, 2.39.

4a: Pale yellow-green solid.

Mp: > 154 °C (dec).

IR ($\mathrm{CH_2Cl_2}$): ν_{CO} ($\mathrm{cm^{-1}}$) 2074 (m), 2 064 (sh), 1 988 (sh), 1 947 (s).

^{1}H NMR ($\mathrm{CDCl_3}$, 500 MHz) δ 3.11 (dd, $^{2}J_{\mathrm{PH}} = {}^{3}J_{\mathrm{PH}} = 5.09$ Hz, 2H, $\mathrm{CH_2}$), 5.28 (d, $^{3}J_{\mathrm{PH}} = 40.52$ Hz, 1H, $\mathrm{H_a}$), 5.64 (d, $^{3}J_{\mathrm{PH}} = 19.53$ Hz, 1H, $\mathrm{H_b}$), 7.27–7.94 (m, 18H, aromatic H′s).

$^{13}\mathrm{C}\{^{1}\mathrm{H}\}$ NMR ($\mathrm{CDCl_3}$, 125.71 MHz) δ 35.72 (dd, $^{1}J_{\mathrm{PC}} = {}^{2}J_{\mathrm{PC}} = 6.85$ Hz, $\mathrm{CH_2}$), 121.75 (d, $^{3}J_{\mathrm{PC}} = 5.28$ Hz, $\mathrm{C_1}$), 128.69 (d, $^{3}J_{\mathrm{PC}} = 9.93$ Hz, $\mathrm{C_3}$), 128.85 (d, $^{3}J_{\mathrm{PC}} = 9.43$ Hz, $\mathrm{C_m}$), 129.96 (d, $^{2}J_{\mathrm{PC}} = 15.41$ Hz, $\mathrm{C_4}$), 130.38 (s, $\mathrm{C_2/C_P}$), 130.77 (d, $^{1}J_{\mathrm{PC}} = 47.64$ Hz, $C\mathrm{{=}CH_2}$), 130.97 (s, $\mathrm{C_2/C_P}$), 132.66 (d, $^{2}J_{\mathrm{PC}} = 12.44$ Hz, $\mathrm{C_o}$), 132.88 (d, $^{2}J_{\mathrm{PC}} = 12.32$ Hz, $\mathrm{C{=}}C\mathrm{H_2}$), 132.6 (d, $^{1}J_{\mathrm{PC}} = 37.33$ Hz, $\mathrm{C_i}$), 138.55 (d, $^{1}J_{\mathrm{PC}} = 40.48$ Hz, $\mathrm{C_\alpha}$), 141.89 (d, $^{2}J_{\mathrm{PC}} = 7.67$ Hz, $\mathrm{C_\beta}$), 204.71 (d, $^{2}J_{\mathrm{PC}} = 9.05$ Hz, 4CO, *cis*), 205.31 (d, $^{2}J_{\mathrm{PC}} = 8.55$ Hz, 4CO′, *cis*), 208.84 (d, $^{2}J_{\mathrm{PC}} = 22.14$ Hz, CO, *trans*), 209.95 (d, $^{2}J_{\mathrm{PC}} = 24.41$ Hz, CO′, *trans*).

$^{31}\mathrm{P}\{^{1}\mathrm{H}\}$ NMR ($\mathrm{CDCl_3}$, 121.66 MHz) δ 28.04 (d, $^{3}J_{\mathrm{PP}} = 6.08$ Hz, $\mathrm{P_A}$), 51.27 (d, $^{3}J_{\mathrm{PP}} = 6.08$ Hz, $\mathrm{P_x}$).

5a: Pale yellow solid.

Mp: > 194 °C (dec).

IR ($\mathrm{CH_2Cl_2}$): ν_{CO} ($\mathrm{cm^{-1}}$) 2 021 (m), 1 926 (sh), 1 907 (s), 1 894 (sh).

^{1}H NMR ($\mathrm{CDCl_3}$, 500 MHz) δ 2.7 (dd, $^{2}J_{\mathrm{PH}} = 18.0$ Hz, $^{3}J_{\mathrm{PH}} = 10.5$ Hz, 2H, $\mathrm{CH_2}$), 5.11 (dd, $^{3}J_{\mathrm{PH}} = 11.5$ Hz, $^{2}J_{\mathrm{HH}} = 4$ Hz, 1H, $\mathrm{H_b}$), 5.6 (ddd, $^{3}J_{\mathrm{PH}} = 24$ Hz, $^{2}J_{\mathrm{HH}} = 4$ Hz, $^{4}J_{\mathrm{PH}} = 0.5$ Hz, 1H, $\mathrm{H_a}$), 7.35–7.94 (m, 18H, aromatic H′s).

$^{13}\mathrm{C}\{^{1}\mathrm{H}\}$ NMR ($\mathrm{CDCl_3}$, 125.71 MHz) δ 41.81 (dd, $^{1}J_{\mathrm{PC}} = 30.8$ Hz, $^{2}J_{\mathrm{PC}} = 17.98$ Hz, $\mathrm{CH_2}$), 121.62 (d, $^{3}J_{\mathrm{PC}} = 4.78$ Hz, $\mathrm{C_1}$), 125.72 (d, $^{2}J_{\mathrm{PC}} = 12.82$ Hz, $\mathrm{C{=}}C\mathrm{H_2}$), 128.26 (d, $^{3}J_{\mathrm{PC}} = 10.06$ Hz, $\mathrm{C_3}$), 128.77 (d, $^{3}J_{\mathrm{PC}} = 9.68$ Hz, $\mathrm{C_m}$), 129.84 (d, $^{2}J_{\mathrm{PC}} = 14.96$ Hz, $\mathrm{C_4}$), 130.28 (d, $^{4}J_{\mathrm{PC}} = 1.89$ Hz, $\mathrm{C_2/C_P}$), 130.97 (d, $^{4}J_{\mathrm{PC}} = 1.76$ Hz, $\mathrm{C_2/C_P}$), 133.09 (d, $^{2}J_{\mathrm{PC}} = 13.32$ Hz, $\mathrm{C_o}$), 133.74 (dd, $^{1}J_{\mathrm{PC}} = 35.33$ Hz, $^{3}J_{\mathrm{PC}} = 1.39$ Hz, $\mathrm{C_i}$), 138.91 (dd, $^{1}J_{\mathrm{PC}} = 37.53$ Hz, $^{3}J_{\mathrm{PC}} = 1.31$ Hz, $\mathrm{C_\alpha}$), 142.2 (d, $^{2}J_{\mathrm{PC}} = 7.17$ Hz, $\mathrm{C_\beta}$), 144.4 (dd, $^{1}J_{\mathrm{PC}} = 29.04$ Hz, $^{2}J_{\mathrm{PC}} = 11.44$ Hz, $C\mathrm{{=}CH_2}$), 210.02 (apparent t, $^{2}J_{\mathrm{PC}} = 9.05$ Hz, CO and CO′, *cis*), 215.21 (dd, $^{2}J_{\mathrm{PC}} = 25.09$ Hz, $^{2}J_{\mathrm{PC}} = 8.3$ Hz, CO, *trans*), 216.25 (dd, $^{2}J_{\mathrm{PC}} = 24.39$ Hz, $^{2}J_{\mathrm{PC}} = 8.93$ Hz, CO′, *trans*).

$^{31}\mathrm{P}\{^{1}\mathrm{H}\}$ NMR ($\mathrm{CDCl_3}$, 121.66 MHz) δ 34.13 (d, $^{2}J_{\mathrm{PP}} = 8.39$ Hz, $\mathrm{P_A}$), 54.79 (d, $^{2}J_{\mathrm{PP}} = 8.39$ Hz, $\mathrm{P_x}$).

Anal Calc for $\mathrm{C_{31}H_{22}MoO_4P_2}$: C, 60.41; H, 3.60. Found: C, 60.28; H, 3.43.

5b: Pale yellow solid.

Mp: > 194 °C (dec).

IR ($\mathrm{CH_2Cl_2}$): ν_{CO} ($\mathrm{cm^{-1}}$) 2 023 (m), 2 010 (sh), 1 928 (sh), 1 909 (s), 1 894 (sh).

^{1}H NMR ($\mathrm{CDCl_3}$, 500 MHz) δ 3.35 (dd, $^{2}J_{\mathrm{PH}} = 19.0$ Hz, $^{3}J_{\mathrm{PH}} = 10.0$ Hz, 2H, $\mathrm{CH_2}$), 4.88 (dd, $^{3}J_{\mathrm{PH}} = 13.0$ Hz, $^{2}J_{\mathrm{HH}} = 3.25$ Hz, 1H, $\mathrm{H_b}$), 5.4 (dd, $^{3}J_{\mathrm{PH}} = 25$ Hz, $^{2}J_{\mathrm{HH}} = 3.25$ Hz, 1H, $\mathrm{H_a}$), 7.36–8.04 (m, 18H, aromatic H′s).

$^{13}\mathrm{C}\{^{1}\mathrm{H}\}$ NMR ($\mathrm{CDCl_3}$, 125.71 MHz) δ 39.59 (dd, $^{1}J_{\mathrm{PC}} = 35.2$ Hz, $^{2}J_{\mathrm{PC}} = 23.51$ Hz, $\mathrm{CH_2}$), 119.66 (d, $^{2}J_{\mathrm{PC}} = 12.41$ Hz, $\mathrm{C{=}}C\mathrm{H_2}$), 121.74 (d, $^{3}J_{\mathrm{PC}} = 4.62$ Hz, $\mathrm{C_1}$), 128.50 (d, $^{3}J_{\mathrm{PC}} = 9.74$ Hz, $\mathrm{C_3}$), 128.71 (d, $^{3}J_{\mathrm{PC}} = 9.13$ Hz, $\mathrm{C_m}$), 130.0 (d, $^{4}J_{\mathrm{PC}} = 1.95$ Hz, $\mathrm{C_2/C_P}$), 130.16 (d, $^{2}J_{\mathrm{PC}} = 15.21$ Hz, $\mathrm{C_4}$), 130.75 (d, $^{4}J_{\mathrm{PC}} = 1.58$ Hz, $\mathrm{C_2/C_P}$), 131.63 (d, $^{2}J_{\mathrm{PC}} = 12.05$ Hz, $\mathrm{C_o}$), 137.34 (dd, $^{1}J_{\mathrm{PC}} = 32.01$ Hz, $^{3}J_{\mathrm{PC}} = 1.22$ Hz, $\mathrm{C_i}$), 138.47 (dd, $^{1}J_{\mathrm{PC}} = 39.07$ Hz, $^{3}J_{\mathrm{PC}} = 1.70$ Hz, $\mathrm{C_\alpha}$), 142.4 (d, $^{2}J_{\mathrm{PC}} = 7.3$ Hz, $\mathrm{C_\beta}$), 145.54 (dd, $^{1}J_{\mathrm{PC}} = 23.67$ Hz, $^{2}J_{\mathrm{PC}} = 14.18$ Hz, $C\mathrm{{=}CH_2}$), 209.43 (apparent t, $^{2}J_{\mathrm{PC}} = 8.74$ Hz, CO and CO′, *cis*), 215.16 (dd, $^{2}J_{\mathrm{PC}} = 24.89$ Hz, $^{2}J_{\mathrm{PC}} = 7.29$ Hz, CO, *trans*), 216.45 (dd, $^{2}J_{\mathrm{PC}} = 23.70$ Hz, $^{2}J_{\mathrm{PC}} = 8.99$ Hz, CO′, *trans*).

$^{31}\mathrm{P}\{^{1}\mathrm{H}\}$ NMR ($\mathrm{CDCl_3}$, 121.66 MHz) δ 41.09 (d, $^{2}J_{\mathrm{PP}} = 10.46$ Hz, $\mathrm{P_A}$), 50.94 (d, $^{2}J_{\mathrm{PP}} = 10.46$ Hz, $\mathrm{P_x}$).

Anal Calc for $\mathrm{C_{31}H_{22}MoO_4P_2}$: C, 60.41; H, 3.60. Found: C, 60.31; H, 3.51.

6a: Pale yellow solid.

Mp: 189–192 °C (dec).

IR ($\mathrm{CH_2Cl_2}$): ν_{CO} ($\mathrm{cm^{-1}}$) 2 023 (s), 1 928 (sh), 1 905 (s).

1H NMR ($\mathrm{CDCl_3}$, 500 MHz) δ 2.00 (ddd, $^{4}J_{\mathrm{PH}} = 6.0$ Hz, $^{3}J_{\mathrm{PH}} = {}^{4}J_{\mathrm{HH}} = 1.5$ Hz, 3H, $\mathrm{CH_3}$), 6.5 (ddq, $^{3}J_{\mathrm{PH}} = 48.49$ Hz, $^{2}J_{\mathrm{PH}} = 7.0$ Hz, $^{4}J_{\mathrm{HH}} = 1.5$ Hz, 1H, $\mathrm{CH_3C{=}C}H$), 7.38–7.98 (m, 18H, aromatic H′s).

$^{13}\mathrm{C}\{^{1}\mathrm{H}\}$ NMR ($\mathrm{CDCl_3}$, 125.71 MHz) δ 20.2 (dd, $^{3}J_{\mathrm{PC}} = 16.59$ Hz, $^{2}J_{\mathrm{PC}} = 1.38$ Hz, $\mathrm{CH_3}$), 121.51 (d, $^{3}J_{\mathrm{PC}} = 4.5$ Hz, $\mathrm{C_1}$), 128.53 (d, $^{3}J_{\mathrm{PC}} = 10.31$ Hz, $\mathrm{C_3}$), 128.68 (d, $^{3}J_{\mathrm{PC}} = 9.03$ Hz, $\mathrm{C_m}$), 129.97 (s, $\mathrm{C_2/C_P}$), 130.31 (d, $^{2}J_{\mathrm{PC}} = 16.22$ Hz, $\mathrm{C_4}$), 130.70 (s, $\mathrm{C_2/C_P}$), 132.16 (d, $^{2}J_{\mathrm{PC}} = 12.44$ Hz, $\mathrm{C_o}$), 135.44 (dd, $^{1}J_{\mathrm{PC}} = 33.81$ Hz, $^{3}J_{\mathrm{PC}} = 2.64$ Hz, $\mathrm{C_i}$), 139.24 (dd, $^{1}J_{\mathrm{PC}} = 41.67$ Hz, $^{3}J_{\mathrm{PC}} = 2.08$ Hz, $\mathrm{C_\alpha}$), 142.82 (d, $^{2}J_{\mathrm{PC}} = 7.79$ Hz, $\mathrm{C_\beta}$), 145.86 (dd, $^{1}J_{\mathrm{PC}} = 39.72$ Hz, $^{2}J_{\mathrm{PC}} = 30.55$ Hz, $\mathrm{CH_3C{=}}C\mathrm{H}$), 156.63 (dd, $^{1}J_{\mathrm{PC}} = 29.67$ Hz, $^{2}J_{\mathrm{PC}} = 24.64$ Hz, $\mathrm{CH_3}C\mathrm{{=}CH}$), 209.47 (apparent t, $^{2}J_{\mathrm{PC}} = 8.17$ Hz, CO and CO′, *cis*), 215.97 (dd, $^{2}J_{\mathrm{PC}} = 26.21$ Hz, $^{2}J_{\mathrm{PC}} = 7.61$ Hz, CO, *trans*), 216.02 (dd, $^{2}J_{\mathrm{PC}} = 23.70$ Hz, $^{2}J_{\mathrm{PC}} = 8.49$ Hz, CO′, *trans*).

$^{31}\mathrm{P}\{^{1}\mathrm{H}\}$ NMR ($\mathrm{CDCl_3}$, 121.66 MHz) δ 46.88 (d, $^{2}J_{\mathrm{PP}} = 4.62$ Hz, $\mathrm{P_A}$), 72.82 (d, $^{2}J_{\mathrm{PP}} = 4.62$ Hz, $\mathrm{P_x}$).

Anal Calc for $\mathrm{C_{31}H_{22}MoO_4P_2}$: C, 60.41; H, 3.60. Found: C, 60.49; H, 3.52.

6b: Pale yellow solid.

Mp: > 222 °C (dec).

IR ($\mathrm{CH_2Cl_2}$): ν_{CO} ($\mathrm{cm^{-1}}$) 2 023 (m), 2 012 (sh), 1 928 (sh), 1 909 (s).

^{1}H NMR ($\mathrm{CDCl_3}$, 500 MHz) δ 1.51 (ddd, $^{4}J_{\mathrm{PH}} = 7.0$ Hz, $^{3}J_{\mathrm{PH}} = {}^{4}J_{\mathrm{HH}} = 1.5$ Hz, 3H, $\mathrm{CH_3}$), 7.3 (ddq,

$^3J_{PH}$ = 49.49 Hz, $^2J_{PH}$ = 5.0 Hz, $^4J_{HH}$ = 1.5 Hz, 1H, $CH_3C{=}C\mathit{H}$), 7.36–7.98 (m, 18H, aromatic H′s).

$^{13}C\{^1H\}$ NMR ($CDCl_3$, 125.71 MHz) δ 17.41 (dd, $^3J_{PC}$ = 15.84 Hz, $^2J_{PC}$ = 1.64 Hz, CH_3), 121.49 (d, $^3J_{PC}$ = 4.53 Hz, C_1), 128.64 (d, $^3J_{PC}$ = 12.32 Hz, C_3), 128.72 (d, $^3J_{PC}$ = 9.43 Hz, C_m), 129.88 (s, C_2/C_P), 130.08 (d, $^2J_{PC}$ = 16.34 Hz, C_4), 130.76 (s, C_2/C_P), 131.71 (d, $^2J_{PC}$ = 12.7 Hz, C_o), 137.65 (dd, $^1J_{PC}$ = 36.83 Hz, $^3J_{PC}$ = 0.5 Hz, C_i), 138.27 (dd, $^1J_{PC}$ = 38.91 Hz, $^3J_{PC}$ = 2.58 Hz, C_α), 142.85 (dd, $^1J_{PC}$ = 39.97 Hz, $^2J_{PC}$ = 37.46 Hz, $CH_3C{=}\mathit{C}H$), 143.3 (d, $^2J_{PC}$ = 7.04 Hz, C_β), 159.5 (dd, $^3J_{PC}$ = 31.43 Hz, $^2J_{PC}$ = 21.12 Hz, $CH_3\mathit{C}{=}CH$), 209.00 (apparent t, $^2J_{PC}$ = 8.8 Hz, CO and CO′, *cis*), 215.34 (dd, $^2J_{PC}$ = 25.9 Hz, $^2J_{PC}$ = 7.91 Hz, CO, *trans*), 216.49 (dd, $^2J_{PC}$ = 24.64 Hz, $^2J_{PC}$ = 8.8 Hz, CO′, *trans*).

$^{31}P\{^1H\}$ NMR ($CDCl_3$, 121.66 MHz) δ 56.34 (d, $^2J_{PP}$ = 4.44 Hz, P_A), 62.33 (d, $^2J_{PP}$ = 4.44 Hz, P_x).

Anal Calc for $C_{31}H_{22}MoO_4P_2$: C, 60.41; H, 3.60. Found: C, 60.25; H, 3.51.

9: Pale yellow solid.

Mp: > 195 °C (dec).

IR (CH_2Cl_2): ν_{CO} (cm^{-1}) 2 022 (m), 1 927 (sh), 1 904 (s).

^1H NMR ($CDCl_3$, 500 MHz) δ 3.21 (dddd, $^2J_{PH}$ = 14.0 Hz, $^4J_{HH}$ = 6.0 Hz, $^3J_{HH}$ = 1.5 Hz, $^4J_{PH}$ = 1.0 Hz, 2H, CH_2), 5.62 (dddt, $^3J_{HH}$ = 12.5 Hz, $^3J_{PH}$ = 6.0 Hz, $^3J_{PH}$ = 3.0 Hz, $^3J_{HH}$ = 1.5 Hz, 1H, $CH_2C\mathit{H}{=}CH$), 6.88 (dddt, $^2J_{PH}$ = 34.49 Hz, $^4J_{PH}$ = 14.0 Hz, $^3J_{HH}$ = 12.5 Hz, $^4J_{HH}$ = 6.0 Hz, 1H, $CH_2CH{=}C\mathit{H}$), 7.2–7.9 (m, 18H, aromatic H′s).

$^{13}C\{^1H\}$ NMR ($CDCl_3$, 125.71 MHz) δ 30.01 (dd, $^1J_{PC}$ = 19.05 Hz, $^3J_{PC}$ = 12.89 Hz, CH_2), 121.74 (d, $^3J_{PC}$ = 4.65 Hz, C_1), 125.66 (dd, $^2J_{PC}$ = 24.83 Hz, $^2J_{PC}$ = 8.49 Hz, $CH_2\mathit{C}H{=}CH$), 128.43 (d, $^3J_{PC}$ = 10.06 Hz, C_3), 128.69 (d, $^3J_{PC}$ = 9.03 Hz, C_m), 129.90 (s, C_2/C_P), 130.03 (d, $^2J_{PC}$ = 16.09 Hz, C_4), 130.35 (s, C_2/C_P), 132.06 (d, $^2J_{PC}$ = 12.32 Hz, C_o), 137.07 (dd, $^1J_{PC}$ = 31.62 Hz, $^3J_{PC}$ = 1.83 Hz, C_i), 140.89 (dd, $^1J_{PC}$ = 43.43 Hz, $^3J_{PC}$ = 2.14 Hz, C_α), 141.59 (d, $^1J_{PC}$ = 10.31 Hz, $CH_2CH{=}\mathit{C}H$), 141.82 (d, $^2J_{PC}$ = 7.67 Hz, C_β), 209.48 (apparent t, $^2J_{PC}$ = 9.12 Hz, CO and CO′, *cis*), 213.37 (dd, $^2J_{PC}$ = 24.64 Hz, $^2J_{PC}$ = 8.8 Hz, CO, *trans*), 214.74 (dd, $^2J_{PC}$ = 22.38 Hz, $^2J_{PC}$ = 8.67 Hz, CO′, *trans*).

$^{31}P\{^1H\}$ NMR ($CDCl_3$, 121.66 MHz) δ 10.91 (d, $^2J_{PP}$ = 32.97 Hz, P_A), 33.61 (d, $^2J_{PP}$ = 32.97 Hz, P_x).

Anal Calc for $C_{31}H_{22}MoO_4P_2$: C, 60.41; H, 3.60. Found: C, 60.33; H, 3.50.

10: White solid.

Mp: > 250 °C (dec).

IR (CH_2Cl_2): ν_{CO} (cm^{-1}) 2 022 (m), 1 932 (sh), 1 906 (s).

^1H NMR ($CDCl_3$, 500 MHz) δ 2.77 (dd, $^2J_{PH}$ = 19.23 Hz, $^3J_{PH}$ = 10.25 Hz, 2H, CH_2), 4.89 (dd, $^3J_{PH}$ = 12.5 Hz, $^2J_{HH}$ = 4.13 Hz, 1H, H_b), 5.05 (dd, $^3J_{PH}$ = 25.25 Hz, $^2J_{HH}$ = 4.13 Hz, 1H, H_a), 7.48–8.03 (m, 16H, aromatic H′s).

$^{13}C\{^1H\}$ NMR ($CDCl_3$, 125.71 MHz) δ 41.79 (dd, $^1J_{PC}$ = 41.79 Hz, $^2J_{PC}$ = 18.92 Hz, CH_2), 119.59 (d, $^2J_{PC}$ = 13.32 Hz, $C{=}\mathit{C}H_2$), 121.74 (d, $^3J_{PC}$ = 4.65 Hz, C_1), 121.9 (d, $^3J_{PC}$ = 4.78 Hz, C_1'), 128.49 (d, $^3J_{PC}$ = 9.80 Hz, C_3), 128.65 (d, $^3J_{PC}$ = 10.06 Hz, C_3'), 129.73 (d, $^2J_{PC}$ = 15.21 Hz, C_4), 130.71 (d, $^2J_{PC}$ = 15.84 Hz, C_4'), 130.84 (s, C_2), 130.90 (s, C_2'), 139.22 (d, $^1J_{PC}$ = 40.35 Hz, C_α), 139.33 (d, $^1J_{PC}$ = 37.84 Hz, C_α'), 142.30 (d, $^2J_{PC}$ = 7.17 Hz, C_β), 142.55 (d, $^2J_{PC}$ = 7.67 Hz, C_β'), 144.63 (dd, $^1J_{PC}$ = 24.64 Hz, $^2J_{PC}$ = 13.07 Hz, $\mathit{C}{=}CH_2$), 209.99 (apparent t, $^2J_{PC}$ = 8.8 Hz, CO and CO′, *cis*), 214.47 (dd, $^2J_{PC}$ = 24.38 Hz, $^2J_{PC}$ = 7.79 Hz, CO, *trans*), 214.51 (dd, $^2J_{PC}$ = 24.32 Hz, $^2J_{PC}$ = 7.86 Hz, CO′, *trans*).

$^{31}P\{^1H\}$ NMR ($CDCl_3$, 202.35 MHz) δ 36.38 (d, $^2J_{PP}$ = 12.45 Hz, P_A), 49.58 (d, $^2J_{PP}$ = 12.45 Hz, P_x).

Anal Calc for $C_{31}H_{20}MoO_4P_2$: C, 60.60; H, 3.28. Found: C, 60.53; H, 3.17.

• *X-ray data collection and processing*

Pale yellow crystals of **3a**, **3b**, **4a**, **5b**, **6a**, **6b**, **8** and **9** were grown by slow diffusion of methanol into a saturated solution of methylene chloride through an ethereal layer at −20 °C. Suitable crystals were mounted on glass fibers and placed on a Siemens P4 diffractometer. Crystal data and details of collection for complexes **3a**, **3b**, **4a** and **8** are given in table X and for complexes **5b**, **6a**, **6b** and **9** are given in table XI. Intensity data were taken in the ω-mode at 298 K with Mo-K_α graphite monochromated radiation (λ = 0.71073 Å). Two check reflections monitored every 100 reflections showed random (< 2%) variation during the

Table X. Crystallographic data for complexes **3a**, **3b**, **4a** and **8**.

	3a	**3b**	**4a**	**8**
Chemical formula	$C_{37}H_{22}Mo_2O_{11}P_2$	$C_{37}H_{22}Mo_2O_{11}P_2$	$C_{37}H_{22}Mo_2O_{11}P_2$	$C_{43}H_{25}Mo_2O_7P_3$
Formula weight	896.4	880.37	880.4	983.42
Crystal system	Triclinic	Orthorhombic	Monoclinic	Monoclinic
Space group	$P\bar{1}$	$Pbca$	$P2_1/n$	$P2_1/n$
a (Å)	11.800(1)	13.965(2)	10.568(2)	10.888(9)
b (Å)	14.004(1)	21.066(2)	27.803(5)	26.790(12)
c (Å)	14.692(1)	25.981(3)	13.154(3)	13.453(5)
α (°)	67.770(10)	90	90	90
β (°)	77.760(10)	90	106.46(2)	92.23(9)
γ (°)	66.000(10)	90	90	90
V (Å^3)	2048.2(4)	7643(2)	3706.1(13)	3921(4)
Z	2	8	4	4
ρ calc (g cm^{-3})	1.453	1.530	1.578	1.590
μ (mm^{-1})	0.744	0.794	0.819	0.813
$R_1(F)$[a]	0.0648	0.0503	0.0782	0.0748
$wR_2(F^2)$[b]	0.1085	0.0838	0.1754	0.1883

[a] $R_1(F) = \sum ||F_o| - |F_c|| / \sum |F_o|$; [b] $wR_2(F^2) = [\sum[W(F_o^2 - F_c^2)^2] / \sum W(F_o^2)^2]^{0.5}$.

Table XI. Crystallographic data for complexes **5b**, **6a**, **6b** and **9**.

	5b	**6a**	**6b**	**9**
Chemical formula	$C_{31}H_{22}MoO_4P_2$	$C_{31}H_{22}MoO_4P_2$	$C_{31}H_{22}MoO_4P_2$	$C_{32}H_{24}Cl_2MoO_4P_2$
Formula weight	616.4	616.37	616.37	701.29
Crystal system	Triclinic	Triclinic	Orthorhombic	Triclinic
Space group	$P\bar{1}$	$P\bar{1}$	$Pbca$	$P\bar{1}$
a (Å)	9.918(1)	10.964(1)	15.671(2)	11.354(1)
b (Å)	10.951(1)	11.707(1)	16.600(2)	11.398(1)
c (Å)	14.968(2)	12.311(2)	21.691(2)	12.014(1)
α (°)	74.04(1)	72.09	90	91.38
β (°)	72.86(1)	68.27	90	105.00
γ (°)	85.02(1)	87.63	90	92.44
V (Å^3)	1385.2(3)	1392.1(3)	5642.8(12)	1499.4(2)
Z	2	2	8	2
ρ calc (g cm^{-3})	1.478	1.470	1.451	1.553
μ (mm^{-1})	0.624	0.621	0.612	0.759
$R_1(F)$[a]	0.0434	0.0265	0.0638	0.0342
$wR_2(F^2)$[b]	0.0700	0.0332	0.1712	0.0433

[a] $R_1(F) = \sum ||F_o| - |F_c|| / \sum |F_o|$; [b] $wR_2(F^2) = [\sum[W(F_o^2 - F_c^2)^2] / \sum W(F_o^2)^2]^{0.5}$.

data collections. The data were corrected for Lorentz, polarization effects and absorption (using an empirical model derived from azimuthal data collections). Scattering factors and corrections for anomalous dispersion were taken from a standard source [18]. Calculations were performed with the Siemens SHELXTL PLUS version 5.0 software package on a personal computer. The structures were solved by direct methods. Anisotropic thermal parameters were assigned to all non-hydrogen atoms. Hydrogen atoms were refined at calculated positions with a riding model in which the C–H vector was fixed at 0.96 Å.

Acknowledgment

We are grateful to the donors of the Petroleum Research Fund, administered by the American Chemical Society, for financial support.

Supplementary material available

X-ray characterization data for complexes **3a**, **3b**, **4a**, **5b**, **6a**, **6b**, **8** and **9** including tables of experimental details, atomic coordinates, thermal parameters, bond distances and bond angles, anisotropic displacement parameters, hydrogen coordinates, and calculated and observed structure factors have been deposited with the British Library, Document Supply Center at Boston Spa, Wetherby, West Yorkshire, LS23 7BQ, UK as Supplementary Publication N° SUP 90452 and are available on request from the Document Supply Centre.

References

1 Carty AJ, Jacobson SE, Simpson RT, Taylor NJ, *J Am Chem Soc* (1975) 97, 7254

2 Taylor NJ, Jacobson SE, Carty AJ, *Inorg Chem* (1975) 14, 2648

3 a) Simpson RT, Jacobson SE, Carty AJ, Mathew M, Palenik GJ, *J Chem Soc, Chem Commun* (1973) 388
  b) Rukachaisirikul T, Arabi S, Hartstock F, Taylor NC, Carty AJ, *Organometallics* (1984) 3, 1587
  c) Carty AJ, Taylor NJ, Johnson DK, *J Am Chem Soc* (1979) 101, 5422

4 Carty AJ, Johnson DK, Jacobson SE, *J Am Chem Soc* (1979) 101, 5612

5 See for example: a) Kagan HB, Dang TP, *J Am Chem Soc* (1972) 94, 6429
  b) Achiwa K, *ibid* (1976) 98, 8265
  c) Wilson ME, Nuzzo RG, Whitesides GM, *ibid* (1978) 100, 2269
  d) Treichel PM, Wong WL, Calabrese JC, *J Organomet Chem* (1978) 159, C20-C24
  e) Brunie S, Mazan J, Langlois N, Kagan HB, *ibid* (1976) 114, 225
  f) Brown JM, Chaloner PA, *J Chem Soc, Chem Commun* (1978) 321
  g) Sanger AR, Tan KG, *Inorg Chim Acta* (1978) 31, L439–L440
  h) Brunner H, Zettlmeier W, Eds, *Handbook Of Enantioselective Catalysis*, VCH, Weinheim, (1993) Vol II

6 Wilson WL, Alcock NW, Alyea EC, Song S, Nelson JH, *Bull Soc Chim Fr* (1993) 130, 673

7 Maitra K, Catalano VJ, Nelson JH, *J Organomet Chem*, (1997) 529, 409

8 Maitra K, Wilson WL, Jemin MM, Yeung C, Rader WS, Redwine KD, Striplin DP, Catalano VJ, Nelson JH, *Synth React Inorg Met Org Chem* (1996) 26(6), 967

9 Garrou PE, *Chem Rev* (1981) 81, 229

10 Crumbliss AL, Topping RJ, In: *Phosphorus-31 NMR Spectroscopy in Stereochemical Analysis*, Verkade JG, Quin LD, Eds, VCH, Deerfield Beach, Florida, (1987) pp 531–557

11 a) Shaw BL, Vessey JP, *J Chem Soc, Dalton Trans* (1992) 1929
  b) Horner L, Ertel I, Ruprecht HD, Belovsky O, *Chem. Ber* (1970) 103, 1582

12 Shaw BL, Vessey JD, *J Chem Soc, Dalton Trans* (1991) 3303

13 Shyu S-G, Calligaris M, Nardin G, Wojcicki A, *J Am Chem Soc* (1987) 109, 3617

14 Keiter RL, Madigan MJ, *Organometallics* (1982) 1, 409

15 Bookham JL, Clegg W, McFarlane W, Raper ES, *J Chem Soc, Dalton Trans* (1993) 3567

16 a) Ueng C-H, Hwang G-Y, *Acta Crystallogr* (1991) C47, 522
b) Ueng C-H, Leu L-C, *Acta Crystallogr* (1991) C47, 752
c) Bernal I, Reisner GM, Dobson GR, Dobson CB, *Inorg Chim Acta* (1986) 121, 199
d) Einstein FWB, Field JS, *J Chem Soc, Dalton Trans* (1975) 1628
e) Uchida T, Uchida Y, Hidai M, Kodama T, *Acta Crystallogr, Sec B* (1975) 31, 1197
f) Sato M, Tatsumi T, Kodama T, Hidai M, Uchida T, Uchida Y, *J Am Chem Soc* (1978) 100, 4447
g) Bishop MW, Chatt J, Dilworth JR, Hursthouse MB, Motevalli M, *J Chem Soc, Dalton Trans* (1979) 1603

17 Linck MH, Nassimbeni LR, *Inorg Nucl Chem Lett* (1973) 9, 1105

18 *International Tables For X-Ray Crystallography*, Reidel, Boston, 1992, Vol C